

Estimates of Accretion Rates of Salt Marsh Islands in Southern New Jersey

Katelyn McGauley



A thesis

submitted to the Faculty of

the Department of Earth and Environmental Sciences

in partial fulfillment

of the requirements for the Bachelor of Science degree of

Earth and Environmental Sciences

Boston College
Morrissey College of Arts and Sciences
Undergraduate Programs

April 2024

Abstract

Salt marshes are an essential ecosystem for connecting nutrients between coastal and land environments, protecting shorelines from erosion, and providing habitat for various species. Anthropogenic climate change causing sea level rise poses threats to salt marshes and the coastal communities nearby. In southern New Jersey, the relative rate of sea level rise (4.21 ± 0.15 mm/yr from 1911-2022; SLR; NOAA, 2023) is greater than the global average (3.4 ± 0.04 mm/yr). In this study, I measure chronologies, bulk density and organic content (loss on ignition, LOI) from cores collected in 2021-22 at four locations in the Seven Mile Island Innovation Lab (SMIIL) in Stone Harbor, New Jersey to determine multidecadal accretion rates. Chronologies are developed from a radionuclide dating analysis (using concentrations of ^{210}Pb , ^{241}Am , ^{137}Cs and ^7Be) following procedures similar to Boyd et al. (2017) and Landis et al. (2016). The accretion rates from 1911-2022 of the four cores analyzed are 4.3 ± 0.2 mm/year, 4.1 ± 0.1 mm/year, 5.2 ± 0.1 mm/yr, and 6.0 ± 0.2 mm/yr, respectively, which are similar to the local SLR rate and are within error of RSLR in Atlantic City. The mean LOI for the 4 four cores is $27.2 \pm 19.0\%$, $21.3 \pm 8.9\%$, $20.2 \pm 7.5\%$ and $14.2 \pm 13.0\%$. The mean dry bulk density for the 4 cores is 437 ± 127 kg/m³, 380 ± 103 kg/m³, 415 ± 88 kg/m³, 657 ± 353 kg/m³. The higher accretion rates of the salt marshes in SMIIL compared to relative sea level rise and consistency with the Sadler Effect indicates that the salt marsh vertical accretion rate is keeping up with increases in sea level rise. Thus, the salt marshes are not in immediate risk for inundation from sea level rise and supports the adaptability and resiliency of the salt marsh ecosystem.

Table of Contents

Abstract	2
Table of Contents	3
List of tables	4
List of figures	4
List of Equations	5
Acknowledgements	6
Introduction	7
Methods	12
Results	17
Discussion	26
Conclusion	30
Appendix	32
References	52

List of Tables

- Table 1.** Core location, date collected, from field site and length used in analysis.
- Table 2.** Visual description of Gull Island 64 cm core for LOI.
- Table 3.** Visual description of Gull Island 85 cm core for geochronology subsampling.
- Table 4.** Visual description of Shark Island Core for LOI.
- Table 5.** Visual description of Shark Island Core for geochronology subsampling.
- Table 6.** Visual description of southeast corner of Gull Island for LOI and geochronology subsampling.
- Table 7.** Visual description of near the Wetlands Institute 2021 for LOI and geochronology subsampling.
- Table 8.** Average LOI, Bulk Density (Equation 1) and Bulk Density (Equation 2) for each coring site.
- Table 9.** Summary of Calculated Accretion Rates for all sampling sites.
- Table 10.** Each site location accretion rates compared to Relative Sea Level Rise and Consistency with the Sadler Effect (Sadler 1981).

List of Figures

- Figure 1.** (A) Map of Southern New Jersey, surrounding water bodies of the study site and locations of NOAA tidal gauges (B) Zoomed in view of the study site and coring location for cores used in analysis.
- Figure 2.** NOAA data of relative rate of SLR in Atlantic City, New Jersey from 1911 to 2023.
- Figure 3.** NOAA data of relative rate of SLR in Cape May, New Jersey from 1967 to 2023.
- Figure 4.** Data from the Gull Island core, including a photograph (a), and depth profiles of LOI, dry bulk density and radionuclide concentrations (b-d). The black bar in d shows the peak of ^{137}Cs and ^{210}Am activity.
- Figure 5.** Data from the Shark Island core, including a photograph (a), and depth profiles of LOI, dry bulk density and radionuclide concentrations (b-d). The black bar in d shows the peak of ^{137}Cs and ^{210}Am activity.
- Figure 6.** Data from the southeast corner of Gull Island core, including a photograph (a), and depth profiles of LOI, dry bulk density and radionuclide concentrations (b-d). The black bar in d shows the peak of ^{137}Cs and ^{210}Am activity.
- Figure 7.** Data from the Near the Wetlands Institute core, including a photograph (a), and depth profiles of LOI, dry bulk density and radionuclide concentrations (b-d). The black bar in d shows the peak of ^{137}Cs and ^{210}Am activity.

List of Equations

Equation 1 Bulk Accretion: Boyd et al. (2017) equation for accretion rate.

Equation 2 Linear Accretion Rate: determined from the CRS (constant rate of supply model) for accretion rate.

Equation 3 Bennett Density: Bennett et al. 1971 equation to calculate bulk density (ρ_d).

Equation 4 Density: Density formula. M = mass of the sample and V =volume

Acknowledgements

Firstly, I would like to thank my thesis advisor, Dr. Noah Snyder, for helping me every step of the way with the completion of my thesis. Noah's continuous support over the course of this project has been invaluable to me. I am incredibly grateful for his guidance and encouragement over the course of this project and my time at BC.

I would also like to thank Josh Landis at the Dartmouth College Radionuclide Fallout Lab in providing analysis on each core sample. Also, I would like to thank Lenore Tedesco at SMILL and Rollins Hagan for field work support.

I have had the privilege to be a part of the Boston College Surfaces Processes Lab Group. I am very grateful to have been in this group as they patiently showed me the ropes of completing a thesis and always offered a helping hand. I would also like to thank Juliana Charslebois-Berg for starting lab work as part of this project over summer 2023 and Dr. Bridget Livers for her assistance throughout the editing process. I owe many thank yous to the Boston College Earth and Environmental Science Department faculty for supporting me over the course of my entire Undergraduate education.

Thank you to ERDC for funding this research.

Finally, thank you to my friends, family and teammates for supporting me throughout my Boston College education.

Introduction

Salt Marsh Ecosystem

Salt marshes play an important role in coastal landscapes as they connect the nutrients between dynamic coastal water environments and land environments. The ecosystem services that they provide are an integral part of the economy, ecosystem health and culture (NOAA 2023; Valiela et al. 2002). Salt marshes provide ecosystem services of carbon and nitrogen sequestration and provide food, refuge, and nursery habitat to various fish and crab species and coastal and migratory birds. These species rely on the health of the coastal marsh systems in order to survive and reproduce (The Wetlands Institute 2019). Furthermore, salt marshes protect shorelines from erosion by acting as a buffer to waves, absorb rainwater to reduce flooding, and improve water quality by filtering runoff (Valiela et al. 2002). Coastal wetlands reduce the effect of hurricanes on coastal communities as they serve as horizontal levees for storm surges. A loss of 1 ha of wetland corresponds to an average \$33,000 increase in storm damage from specific storms (Costanza, 2008).

However, salt marshes and their beneficial impact to ecosystem health and coastal protection are threatened by climate change, most specifically sea level rise (SLR). Due to sea level rise, coastal wetlands are declining rapidly. Studies have indicated that a 1 m increase in SLR will result in 96% decrease of North America's coastal wetlands (Blankespoor et al. 2014). In addition to the risk associated with sea level rise, land subsidence from glacial isostatic adjustment and groundwater withdrawal, particularly prevalent on the United States East Coast, increases the relative sea level rise and increases the risk of inundation (Ohenhen et al. 2024). In the US, the Environmental Protection Agency (EPA) has evaluated the vulnerability of salt marshes and management practices for maintaining the health of the fragile ecosystem (EPA 2023). If the ocean inundates the marshes, the marsh would lose its biological and ecological

ability to grow due to a lack of oxygen (NSF 2013). Frequent flooding cuts off the oxygen supply to vegetation in the marsh, causing plants to die and the marsh to “disappear” as sea level continues to rise (NSF 2013).

Understanding the coastal processes of vertical accretion in salt marshes provides information about the impact of SLR on salt marshes and natural adaptations to changing environments. As a dynamic ecosystem, salt marshes can grow overtime from organic and inorganic material accumulation. Vertical growth, or marsh accretion, can be attributed to the deposition of suspended sediment and organic matter from plants. The three factors that primarily drive marsh accretion are biological productivity, sediment supply and sea level rise (Weis et al. 2016). The objective of this study is to analyze accretion rates of salt marshes to better understand if marshes are vertically accumulating at the rate of sea level rise.

Radionuclide Dating

The four short-lived radioisotopes that satisfy the criteria for measuring sedimentary dynamics over the past 100 to 150 years are ^7Be , ^{241}Am , ^{137}Cs and ^{210}Pb . Short-lived radioisotopes can provide information about accretion of salt marshes. Beryllium-7 is a naturally occurring radioisotope that is transferred through precipitation from the atmosphere to Earth. Due to a half life of 53 days, ^7Be is effective in dating sediment less than 1 year old and will not be used because cores were collected over a year ago. Both ^{241}Am and ^{137}Cs are produced by nuclear weapons testing, and measurable environmental signals began in 1952 and peaked in 1963 (Landis et al. 2016). Lead-210 accumulates in marsh peat layers from global distribution in the atmosphere and enters the soil during surficial exposure and upon sequential burial of each ^{210}Pb layer (Landis et al. 2016). The half life ^{210}Pb is consistent through time at 22.3 years, making it ideal for ecosystem study (USGS 1998). Supported ^{210}Pb is from natural processes

from the decay of ^{226}Ra which is eroded by rocks and incorporated into sediment. Unsupported ^{210}Pb is from the decay of ^{222}Rn in the atmosphere. In addition to dating from the decay of ^{210}Pb , peaks in concentration of ^{137}Cs and ^{241}Am correspond to the bomb peak of 1963 due to extensive above ground nuclear weapons testing. The peaks of ^{137}Cs and ^{241}Am and dating of ^{210}Pb were used to determine a bomb peak year corresponding depth in the core (Landis et al. 2016).

Study Site

All the study sites are located in Cape May County in the Cape May Wetlands Wildlife Management Area and fall under the jurisdiction of the New Jersey Division of Fish and Wildlife. The field sites are situated within the 62.16 km² Seven Mile Island Innovation Lab (SMIL) in Stone Harbor, New Jersey, which includes tidal marshes, coastal lagoons, bays and tidal inlets (Figure 1B). The site provides irreplaceable habitat for various species of wildlife, including threatened and endangered species, as well as being a carbon sink. SMIL is in collaboration between the Army Corp of Engineers (USACE), the State of New Jersey, the Wetlands Institute (TWI) and the USACE Engineer Research and Development Center (ERDC) that seeks to advance research in marsh restoration techniques.

The four sites where sediment cores were collected from are Shark Island, the middle of Gull Island, the southeast corner of Gull Island and from near The Wetlands Institute dock (Figure 1B). Gull Island has an area of 1.2 km² and a perimeter of 5.43 km. Shark Island has an area of 3.56 km² and a perimeter of 9.39 km. In this system, mineral and organic sediment controls the vertical accumulation in the area. Mineral sediment comes from beach channels and the erosion of salt marsh islands as there are no river sources into the system. Organic sediment comes from vegetation on the salt marsh islands (Zeff et al. 1988).

Sea Level Record

The relative sea level rise (RSLR) is determined by NOAA through tide gauges and satellite altimeters to measure the height of the water relative to a specific point on land. Therefore, the NOAA model for sea level rise includes the impact of subsidence and rising global sea level and provides a comprehensive model of sea level rise for comparison to accretion rates for this study (NOAA 2023).

The beginning of the sea level record in southern New Jersey began in 1911. The site in southern New Jersey is particularly of interest due to the local sea level increase in Atlantic City (4.21 ± 0.15 mm/year) and in Cape May (4.99 ± 0.44 mm/yr) being higher than the global average (3.4 ± 0.04 mm/yr) (Blackwood, n.d.) (Figure 2 and 3). The difference is largely attributed to land subsidence in New Jersey due to glacial isostatic adjustment and anthropogenic factors, such as groundwater extraction and sediment compaction (Ohenhen et al. 2024). In local areas around Atlantic City, the rate of land subsidence reaches 3 mm/year and is among the highest on the United States east coast (Ohenhen et al. 2024).

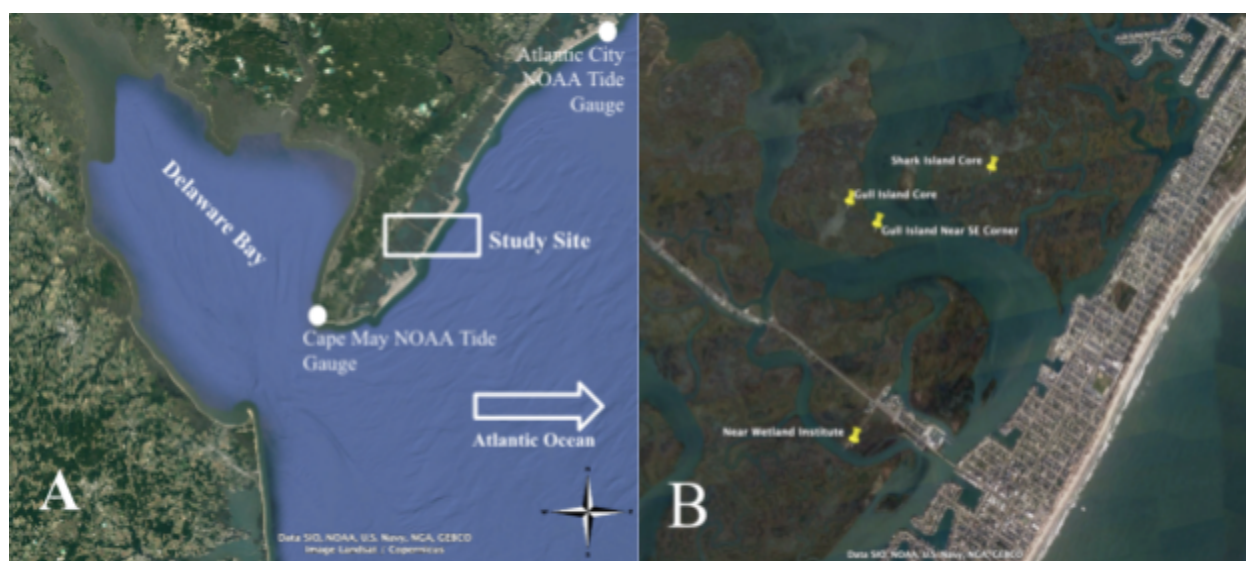


Figure 1. (A) Map of southern New Jersey, surrounding water bodies of the study site and locations of NOAA tidal gauges. (B) Zoomed in view of the study site and coring location for cores used in analysis.

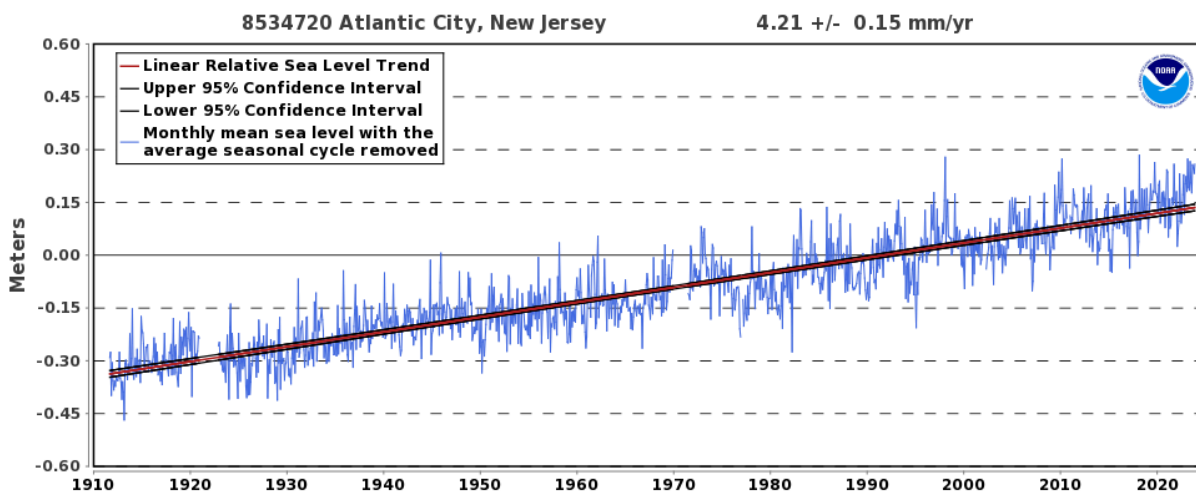


Figure 2. NOAA data of relative rate of SLR in Atlantic City, New Jersey from 1911 to 2023.

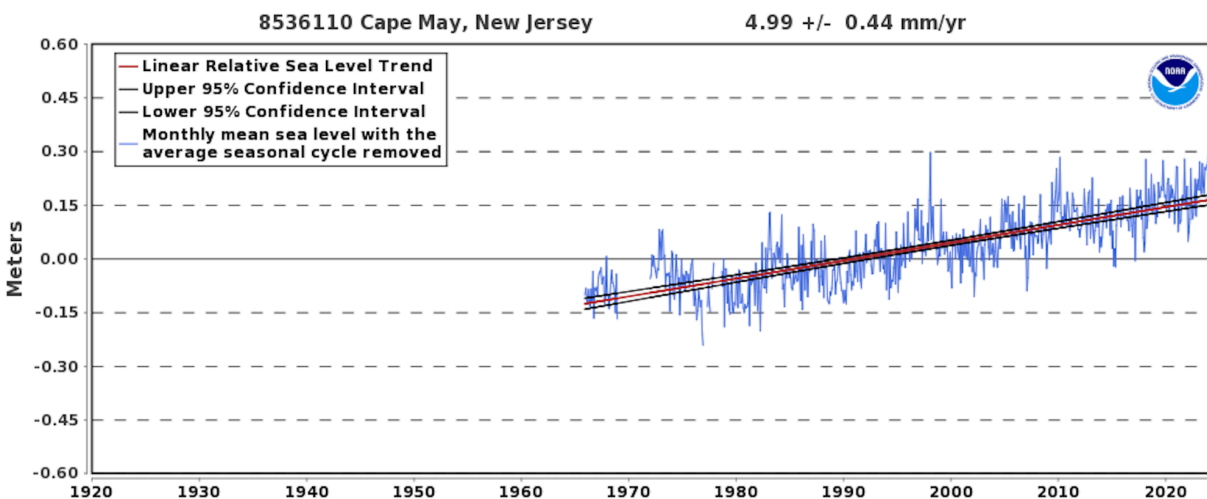


Figure 3. NOAA data of relative rate of SLR in Cape May, New Jersey from 1967 to 2023.

Objectives

The purpose of this project is to develop chronologies for 4 salt marsh cores from sites in SMIL, as well as measure organic content and bulk density. The project is a continuation from work in a 2022-2023 Senior Research Seminar as outlined in Charlebois-Berg et al. (2023), which analyzed a salt marsh core from the middle of Gull Island (Figure 1B). The development of the chronologies from three additional cores from Shark Island, the southeast corner of Gull Island and near the Wetlands Institute, and comparison of the cores, will allow for a better

understanding of accretion rates of salt marsh islands in SMIL. Furthermore, the comparison will provide a comprehensive perspective on how sea level rise affects the SMIL salt marshes. The objectives of this project are: (1) develop chronologies for four salt marsh cores from three islands in southern New Jersey using radioisotopic analyses, as well as measure organic content and bulk density for the cores; and (2) compare findings to the rate of the relative sea level rise in order to understand the inundation risk.

The hypothesis from research on Gull Island was that the accretion rate at SMIL would be lower than the rate of RSLR, and consequently, the marsh islands would be at heightened risk for inundation. The hypothesis for research about Gull Island was not supported by the results (Charlebois-Berg et al. 2023). The research determined that the multidecadal accretion rate for Gull Island was 4.3 mm/year and RSLR at 4.17 mm/year from NOAA data from 1911-2021 in southern New Jersey (Figure 2). Therefore, it was found that Gull Island marsh accretion from mineral sediment and organic matter is keeping up with the rate of SLR. Between 2021 and 2023, the NOAA record for sea level rise increased from 4.17 mm/yr to 4.21 ± 0.15 mm/yr (Charlebois-Berg et al. (2023). Even so, I hypothesize that the accretion rates at Shark Island, Gull Island and near the Wetland Institute are the same or higher than the rate of local sea level rise, and do not have high risk for inundation.

Methods

Field Collection and Sampling Methods

Sediment cores were collected by pushing a 2 m long by 7.5 cm diameter aluminum tube and then cut down to final sampling size into the salt marshes on Gull Island, Shark Island and near the Wetlands Institute dock (Figure 1B). Two cores each were collected from Gull and Shark islands in October 2022. The lengths of the cores from Gull Island were 85 cm and 64 cm,

respectively. The lengths of the Shark Island cores were 82 cm and 91 cm, respectively. The cores from the southeast corner of Gull Island and near the Wetland Institute were collected in October 2021. The length of the SE corner of Gull Island core was 96 cm and the core near the Wetland Institute was 121 cm (Table 1). All the cores were vertically cut in half at the time of collection at the Wetlands Institute then later split at the laboratory at Boston College. The cores were stored in a cold room at Boston College.

Core Name	Core Location	Date Collected	Length of Sediment (cm)	Latitude and Longitude
GC-1-22-1	Gull Island	October 16, 2022	85	39.075973, -74.775485
GC-1-22-2	Gull Island	October 16, 2022	64	39.075973, -74.775485
GC-2-22-1	Shark Island	October 16, 2022	82	39.078727, -74.760563
GC-2-22-2	Shark Island	October 16, 2022	91	39.078727, -74.760563
GULL-2021-1	Southeast Corner of Gull Island	October 23, 2021	81	39.07415, -74.77258
TWI-2021-1	Near the Wetlands Institute Dock	October 23, 2021	121	39.05771, -74.77464

Table 1. Core location, date collected, from field site and length used in analysis.

In the laboratory, cores were visually analyzed for differences with depth. The 64 cm Gull Island core, 82 cm Shark Island core, the SE corner Gull Island core and the Wetlands Institute dock were used to determine the loss of ignition (LOI) and bulk density.

Radionuclide Dating

For subsampling for radionuclide dating, the 85 cm Gull Island core and 91 cm Shark Island core were cut into 3 cm intervals. The southeast corner of Gull Island and Wetlands Institute cores were cut into 4 cm intervals after LOI and bulk density samples were taken. The core sections were placed on labeled aluminum pans, weighed and placed in the drying oven at 60°C for 48 hours to dry out. The dried sediment was weighed, mashed and packed into plastic containers. All the samples were mailed to the Fallout RadioNuclide Analytics Lab at Dartmouth College for radionuclide measurements (Landis, 2023).

In collaboration with the Department of Earth Science at Dartmouth College, and following the methods of Landis et al. (2016): a gamma spectrometer takes radionuclide measurements in order to compare the concentration of ^{210}Pb in relation to its depth in the sediment. The Constant Rate of Supply model (CRS) and the Linked Radionuclide Accumulation model (LRC) are empirical models for estimating age from concurrent measurements of radionuclide activity of ^{210}Pb . Measurements of ^{210}Pb are processed in CRS and LRC age models to correspond various depths with an age and calendar year.

In addition to ^{210}Pb , ^{137}Cs and ^{241}Am data was collected and measured, and uses ^{137}Cs as the primary independent marker. The age determination with the peak in ^{137}Cs and ^{241}Am is compared to the ^{210}Pb age model in order to determine the radionuclide fallout date. The three assumptions for ^{210}Pb and ^{137}Cs dating methods are: (1) particle mixing from a burrowing organism has not altered the initial age-depth relationship; (2) the radionuclide is chemically static; (3) the sedimentary record is complete and not altered by significant non-deposition or erosion (Boyd et al. 2017).

The age models of ^{210}Pb , ^{241}Am and ^{137}Cs were used to calculate bulk accretion and linear accretion rates are based on methods outlined in Boyd et al. (2017). Bulk and linear accretion

rates are calculated using ^{210}Pb chronology and testing with the ^{137}Cs and ^{241}Am chronology. The accretion rates were measured from 3 different start points: the oldest date in the core, 1911 as marked by the beginning of the sea level record and from the year of ^{241}Am and ^{137}Cs peak, based on ^{210}Pb chronology. Both calculated accretion rates are used to determine the average rate of accumulation of sediment in the system and, on longer time scales, consistency with the Sadler Effect (Sadler 1981).

Two different equations were used to determine accretion rates. Bulk accretion rate from Boyd et al. (2017) is the overall accumulated mass depth at a given time and divided by the number of years in that interval (Equation 1). Standard deviation can not be calculated for bulk accretion rate (Equation 1). For linear rates, the rate is represented by each subsample in an interval, which is calculated by the thickness of the subsample divided by the time in the interval based on the ^{210}Pb age model (Equation 2). Then, standard deviation for linear accretion is calculated.

$$\text{Bulk Accretion Rate} = \frac{\text{Depth of a Specific Interval}}{\text{Total Number of Years Since that Interval}}$$

Equation 1 Bulk Accretion: Boyd et al. (2017) equation for accretion rate.

$$\text{Linear Accretion Rate} = \frac{\text{Rate Represented by Each Subsample}}{\text{Total Time in that Interval}}$$

Equation 2 Linear Accretion Rate: determined from the CRS (constant rate of supply model) for accretion rate.

Loss on Ignition

On each core, 2 cm³ samples were extracted by a plastic syringe every 2 cm of the core. Each 2 cm³ sample was placed into tared crucibles and weighed to determine the weight of the wet sediment. Samples were weighed after they were placed in the oven at 100°C for 24 hours; water content was determined by the difference between wet and dry weights of oven-dried samples. After they cooled, LOI was performed in order to calculate the organic content. Samples were weighed before and after they were placed in the muffle furnace to burn at 550-600°C for 4 hours. The difference between the weight before and after the oven is the organic content.

Bulk Density

Bulk density refers to the total of the density of the organic and inorganic sediment. The physical soil properties of the cores were similar to those outlined in Boyd et al. (2017).

Both the dry bulk density equation in Bennett et al. (1971) and the traditional method of density were used in order to account for an imprecise volume measurement. First, in order to calculate the bulk density (ρ_d), the water and organic matter content were found for each sample as described in the previous section. Assumptions were made about density of seawater (ρ), and unconsolidated solids (ρ_s) as made in Boyd et al. (2017). Assumed density of seawater (ρ) and density (ρ_d) for minerals and organic matter were 1020 kg/m³, 2610 kg/m³ and 1140 kg/m³, respectively. Figures were created similarly to Boyd et al. (2017) for all marsh island cores to describe sediment content by depth and relative inorganic and organic matter in the marshes.

$$\rho_d = \frac{1-W}{\frac{W}{\rho} + \frac{1-W}{\rho_s}}$$

Equation 3 Bennett Density: Bennett et al. 1971 equation to calculate bulk density (ρ_d).

$$\rho_d = \frac{M}{V}$$

Equation 4 Density: Density formula. M= mass of the sample and V=volume

Results

Each core was visually analyzed and described before subsampling (Tables 2-7). When measured in the lab, the core sampled from near the Wetlands Institute was 118 cm which is 2 cm shorter to when it was first collected due to compaction (Table 7).

Depth (cm)	Visual Description
0-2.5	Empty, no sample
2.5-9	Light brown layer mud, vegetation
9-22	Blacker mud, vegetation
22-39	Transformation from brown mud with vegetation to gray mud with vegetation
39-64	Gray mud with potential active roots at 51 cm

Table 2. Visual description of Gull Island 64 cm core for LOI.

Depth (cm)	Visual Description
0-9	Light brown peat with active roots
9-17	Black/dark brown mud, black vegetation, active roots
17-22	Brown mud, Abundant vegetation
22-36	Gray mud, sparse vegetation
36-85	Mixture of dark brown mud and abundant vegetation

Table 3. Visual description of Gull Island 85 cm core for geochronology subsampling.

Depth (cm)	Visual Description
0-16	brown peat with macroscopic (obvious large pieces of vegetation), not well compacted
16-27	brown peat transitioning downward to grayer peat
27-57	gray-brown peat
57-77	gray-brown peat
77-80	gray peat
80-87	dark brown peat

Table 4. Visual description of Shark Island Core for LOI.

Depth (cm)	Visual Description
0-27	brown peat, gradually gets darker w/ depth (brown to dark brown)
27-38	gray-brown color peat
38-76	even more decomposed, peat, smaller organics, transitioning from gray to light brown color
76-78	more macro-scale organic layer that is almost reddish-brown
79-82	light brown decomposed organics

Table 5. Visual description of Shark Island Core for geochronology subsampling.

Depth (cm)	Visual Description
0-4	black peat with large pieces of grass and roots
4-15	Brown peat
15-18	Darker brown to black peat
18-28	Brown peat
28-46	Reddish-brown peat
46-71	brown peat
71-79	Brown peat
79-81	Gray-brown peat

Table 6. Visual description of southeast corner of Gull Island for LOI and geochronology subsampling.

Depth (cm)	Visual Description
0-22	Brown Peat
22-26.0	Dark Grey/black peat
26.0-26.2	Possible sand layer
26.2-66	Gray peat and some mud
66-98	Muddy grey peat
98-118	Mud and finer organic material

Table 7. Visual description of near the Wetlands Institute 2021 for LOI and geochronology subsampling.

Organic Content and Bulk Density

Table 8 summarizes LOI, average bulk density and standard deviations for the four analyzed cores. Average bulk density using Bennett et al. (1971) method (Equation 3) and the standard density equation (Equation 4) were higher near the Wetlands Institute than the Shark and Gull Island cores (Table 8). High bulk density may be due to location of the site in relation to the channel.

LOI calculations reveal the organic content of the core. At all of the core sites, the organic and inorganic content fluctuates with depth (Figure 4-7). The Gull Island core has the highest LOI ($27.12 \pm 8.195\%$) and the Wetlands Institute core has the lowest LOI ($14.22 \pm 13.080\%$) (Table 8). On Gull Island, organic content peaks at 40 cm and 49 cm and it is relatively low at the top of the core (Figure 3). On the southeast corner of Gull Island, organic content peaks between 6-8 cm and decreases with depth (Figure 5). Organic content near the Wetlands Institute peaks at 4-6 cm, and decreases with depth except for fluctuations 18-25 cm (Figure 6). Organic content decreases with depth on Shark Island (Figure 4).

Core Location	Average LOI	Standard Deviation LOI	Average Bulk Density Bennett et al. 2017 Equation (kg/m ³)	Standard Deviation Average Bulk Density Bennett et al. 2017 Equation (kg/m ³)	Average Bulk Density (kg/m ³)	Standard Deviation Average Bulk Density (kg/m ³)
Gull Island	27.12%	8.195%	435.9	127.30	464.6	142.40
Shark Island	21.33%	8.999%	380.4	102.90	336.5	91.12
Southeast Corner of Gull Island	20.15%	7.752%	414.5	88.27	380.9	85.57
Near the Wetlands Institute	14.22%	13.080%	656.9	353.45	641.5	397.60

Table 8. Average LOI, Bulk Density (Equation 1) and Bulk Density (Equation 2) for each coring site.

Marsh Accretion Rates

Calculations from the Radioisotopic Lab at Dartmouth College on CRS accretion rate, ¹³⁷Cs and ²⁴¹Am peak year and LOI and bulk density provide an overview of the key findings for all 4 sample locations.

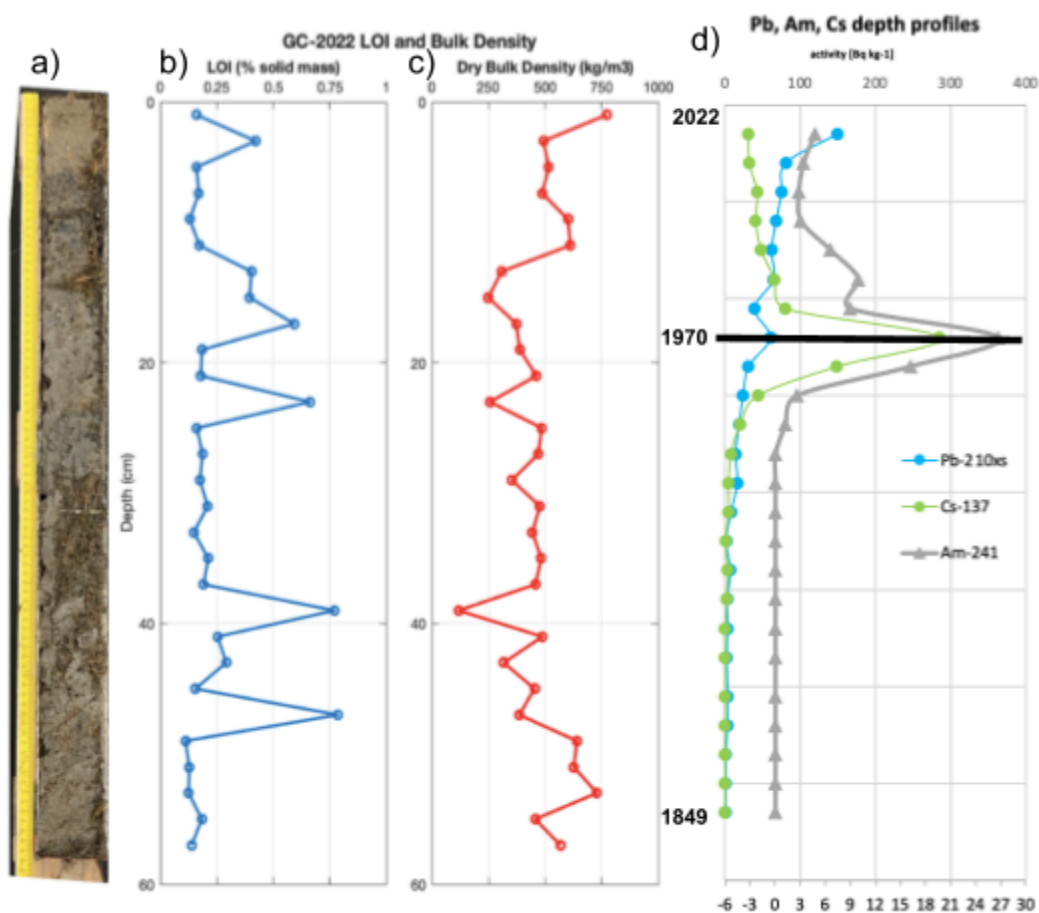


Figure 4. Data from the Gull Island core, including a photograph (a), and depth profiles of LOI, dry bulk density and radionuclide concentrations (b-d). The black bar in d shows the peak of ^{137}Cs and ^{210}Am activity.

The ^{210}Pb decay model follows a downward exponential trend through time for all cores (Figures 4-7). For the Gull Island core, ^{137}Cs and ^{241}Am deposition peaks at a depth of 18-19 cm, which corresponds to a peak year of 1970, according to the ^{210}Pb age model (Figure 4). The peak year of 1970 varies slightly from 1963, which suggests some timescale of sediment mixing at this site. The bottom of the Gull Island core was dated to 1740 according to the ^{210}Pb age model. The Shark Island core ^{137}Cs and ^{241}Am deposition peaks at 22.5 cm depth and corresponds to the 1964 peak year based on the ^{210}Pb model which is a one year difference from the 1963 bomb

peak year. According to the ^{210}Pb age model, the date of the bottom of the core was 1823. The southeast corner of Gull Island core ^{137}Cs and ^{241}Am deposition peaks at 24-28 cm depth and corresponds to a 1966 peak year which is a 3 year difference from the 1963 bomb peak year. The beginning of the marsh record starts in 1774. The Wetlands Institute core ^{137}Cs and ^{241}Am deposition peaks at 28-32 cm depth and corresponds to the 1969 peak year which is a 6 year difference from the 1963 bomb peak year. The date of the bottom of the core was 1802 according to the ^{210}Pb age model.

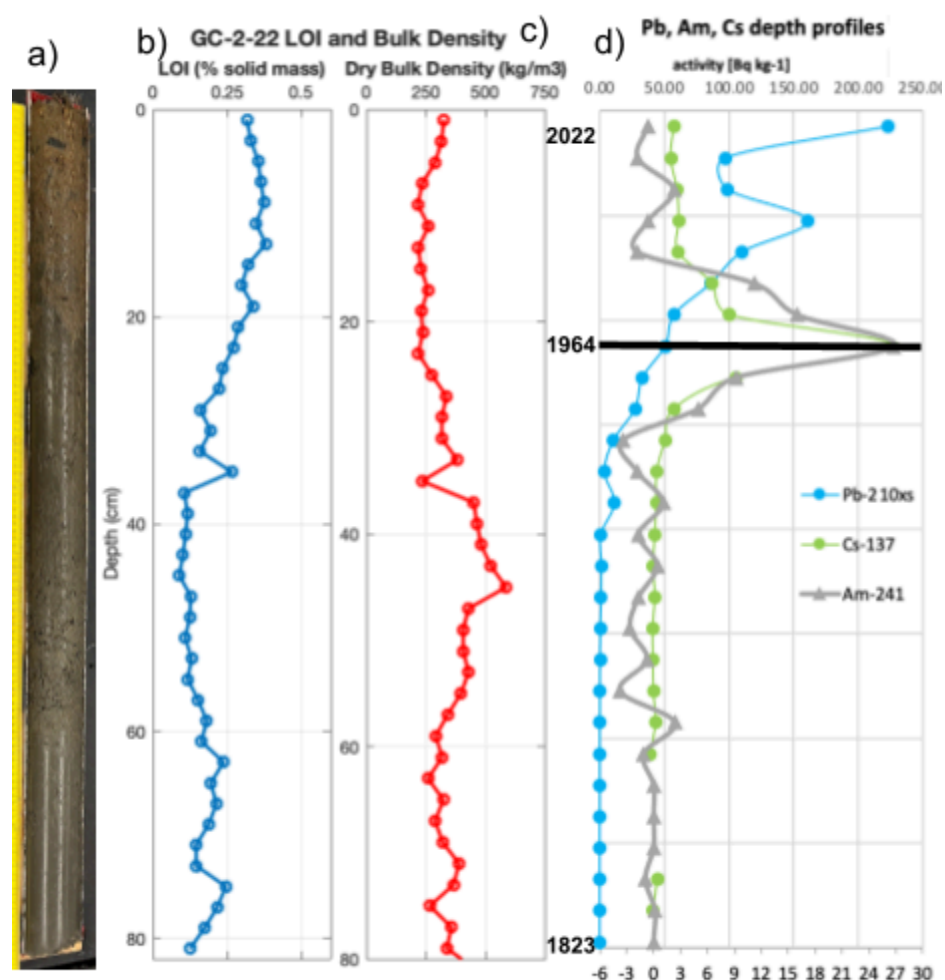


Figure 5 Data from the Shark Island core, including a photograph (a), and depth profiles of LOI, dry bulk density and radionuclide concentrations (b-d). The black bar in d shows the peak of ^{137}Cs and ^{210}Am activity.

Table 9 summarizes the accretion rates for all sites over three different time intervals (Table 9). The highest accretion rates between all three time scales is the near the Wetlands Institute (Table 9). The lowest accretion rate between the core collection date and the bomb peak year is Gull Island (4.3 ± 0.2 mm/yr and 4.4 mm/yr) (Table 9). The lowest accretion rate for the entire core is Shark Island (2.8 ± 0.25 mm/yr and 2.3 mm/yr) (Table 9).

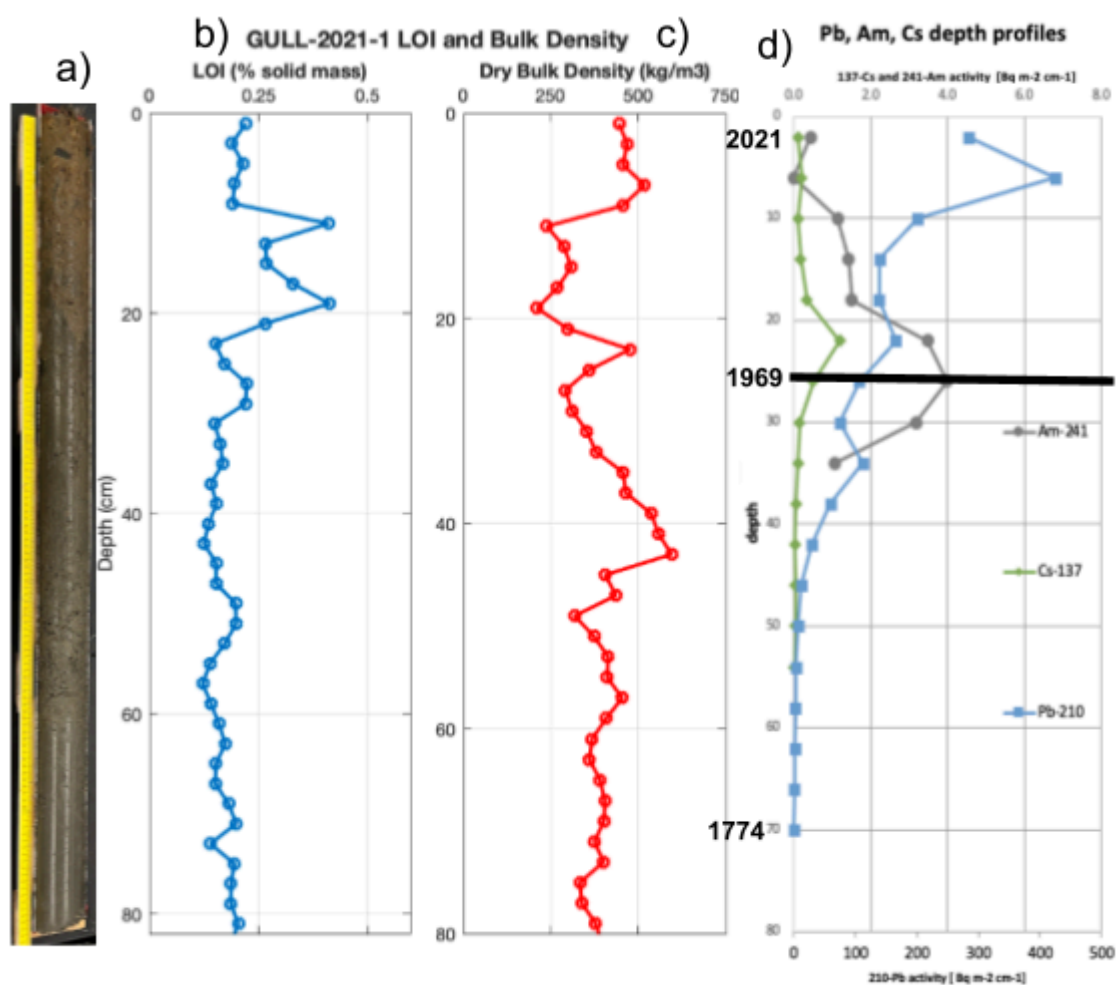


Figure 6. Data from the southeast corner of Gull Island core, including a photograph (a), and depth profiles of LOI, dry bulk density and radionuclide concentrations (b-d). The black bar in d shows the peak of ¹³⁷Cs and ²⁴¹Am activity.

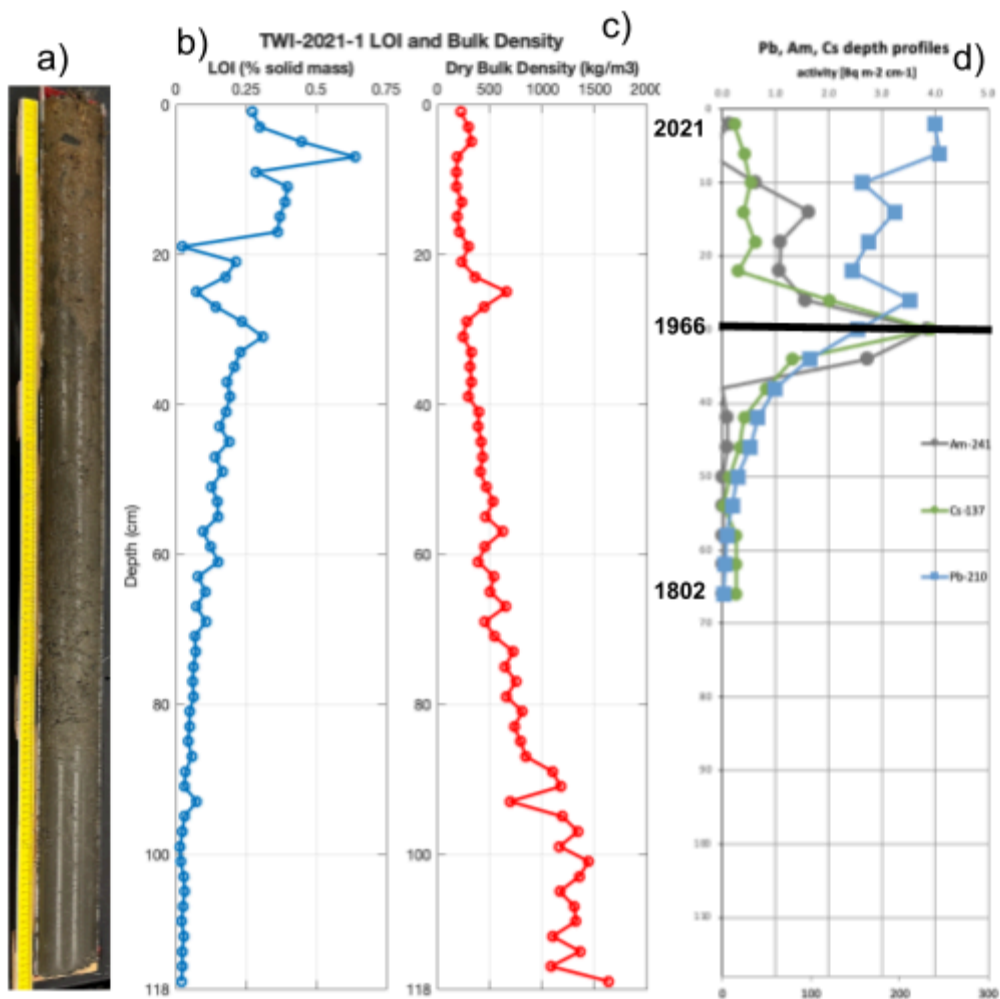


Figure 7. Data from the near the Wetlands Institute core, including a photograph (a), and depth profiles of LOI, dry bulk density and radionuclide concentrations (b-d). The black bar in d shows the peak of ^{137}Cs and ^{210}Am activity.

Core Location	Accretion Model	From the year of ^{241}Am and ^{137}Cs Peak, based on ^{210}Pb chronology (mm/yr)	From 1911 beginning of RSLR record (mm/yr)	From oldest date of core (mm/yr)
Gull Island	Linear Accretion	4.3 ± 0.2	4.7 ± 0.3	5.1 ± 0.3
	Bulk Accretion	4.4	4.3	4.1
Shark Island	Linear Accretion	4.1 ± 0.1	3.8 ± 0.1	2.8 ± 0.1
	Bulk Accretion	3.8	3.3	2.3
SE Corner of Gull Island	Linear Accretion	5.2 ± 0.1	4.4 ± 0.2	3.4 ± 0.2
	Bulk Accretion	5.9	4.9	2.8
Near The Wetlands Institute	Linear Accretion	6.0 ± 0.2	4.9 ± 0.3	4.0 ± 0.3
	Bulk Accretion	6.8	5.1	3.0
Mean Values	Linear Accretion	4.9 ± 0.2	4.2 ± 0.2	3.8 ± 0.2
	Bulk Accretion	5.2	4.4	3.1

Table 9. Summary of Calculated Accretion Rates for all sampling sites.

Discussion

Accretion Rates

Over long time intervals, the rate of marsh accretion should be very similar to that of RSLR because flood-induced stress affects biological production through the biophysical feedback between sediment trapping and accretion (Boyd et al. 2017). The mean accretion rate of this analysis since 1963 (4.9 ± 0.2 mm/year and 5.2 mm/year) is very similar to the rate of RSLR (4.21 ± 0.2 mm/year) in the area, suggesting that SLR is most likely the limiting factor on accretion rate (Figure 2). The ability for a marsh accretion rate to match sea level rise is

dependent on sufficient sediment availability and biologically productive vegetation (Weis et al. 2016). However, with evidence that sea level rise is accelerating, the ability for marshes to continue accreting at increasing rates is thrown into question.

Average LOI and bulk density are similar for the central Gull Island, southeast corner of Gull Island and Shark Island cores (Figures 3-6; Table 8). The similarity demonstrates there are similar percentages of organic matter between each coring location. Low average LOI and high bulk density in the core near the Wetland Institute demonstrates a different percent of organic matter and differing composition than the other three cores. This could be because it is located closer to a main channel than the other core sites and therefore may receive more inorganic sedimentation (Table 8).

The core near the Wetland Institute has a sand layer at 26.0-26.2 cm depth (Table 7). ^{210}Pb age models from radionuclide dating indicate this layer was deposited in 1985, corresponding to the year when Hurricane Gloria hit the New Jersey coast. The deposition of sand indicates a washover from flooding from episodic sediment deposition from a high energy storm (Groot 2011). The corresponding sand layer at 26 cm depth, age model estimate, and year of a known storm event supports the confidence in the radionuclide model.

Variation in ^{137}Cs and ^{241}Am Peak Year

Globally, ^{137}Cs and ^{241}Am concentrations peaked in 1963. Each of the four cores show clear, coincident peaks in these activities (Figures 4-7). However, based on the ^{210}Pb age model, these layers date to 1964-1970 (Figures 4-7; Table 9). The offset between peaks in ^{137}Cs and ^{241}Am and the bomb peak year from the ^{210}Pb model indicates movement and sloshing of sediment in the system until it settled. The SMILL site has no direct river source to introduce sediment into the system. Therefore, it can be concluded that sediment and organic material for

lateral deposition is from tides and erosion from subsequent accretion from other marshes. This offset may also be attributed to uncertainty in the data. Possible sources of uncertainty in the data is contamination during core extraction or during subsampling the core, or the size of the subsample. In some cases, the material from a subsample did not fill the plastic container provided by Dartmouth, which affects measurement. Even with possible uncertainty, (1) levels of ^{137}Cs and ^{241}Am do not return to zero at the top of any of the cores and; (2) age determinations for all cores was post 1963 rather than before the 1963 bomb strike. The two factors demonstrate it is likely that old sediment is recycled in the system.

Comparison

The goal of this study was to compare the accretion rates of different salt marsh islands in the SMILL in southern New Jersey and determine if the marsh accretion rates were keeping up with the rate of RSLR. The hypothesis that the salt marsh accretion rates are similar to higher compared to relative sea level rise is supported by the findings of this research. However, the findings suggest that the salt marsh islands differ in accretion rate compared to RSLR in Atlantic City (4.21 ± 0.2 mm/yr). The accretion rate from 1911 to the core extraction year on Gull Island (4.7 ± 0.3 mm/yr), Shark Island (3.8 ± 0.2 mm/yr), the southeast corner of Gull Island (4.4 ± 0.2 mm/yr) and near the Wetlands Institute (4.9 ± 0.3 mm/yr) overlap within error of RSLR from Atlantic City and is similar to the relative sea level rise (Table 9). Higher accretion rates indicate marsh is exceeding sea level rise and is not at any risk for inundation. The difference in accretion rates in location demonstrates the dynamic nature of the ecosystem and difference in sediment and accretion based on location. Even with differing accretion rates, the findings from all four cores demonstrates that salt marsh island accretion is keeping up with local RSLR (Table 10).

The Sadler Effect describes variation in accretion rates over time. Cores consistent with the Sadler Effect record higher accretion rates in shorter time scales compared to a long time scale. Cores that record a longer time scale will have a slower accretion rate because of compaction, intervals of non-deposition and time. Compaction of the bottom of the cores increases density (Sadler et al. 1981). Thus, compaction results in a higher accretion rate for shorter time scales. Secondly, shorter time scales reduce the size of the denominator when calculating accretion rate. A lower denominator results in a higher overall accretion rate compared to a larger time scale and higher denominator to calculate accretion rate.

The Shark Island, southeast corner of Gull Island and near the Wetlands Institute cores are all consistent with the Sadler Effect (Table 10). The Gull Island core is inconsistent with the Sadler Effect as it does not show higher accretion rates on shorter time scales (Table 10).

Higher accretion rates on shorter time scales demonstrates that the salt marsh system is keeping up with RSLR as it accelerates in recent decades. The SMIL site cores demonstrate salt marshes are keeping up with sea level rise, especially in recent years when sea level rise rates are increasing. Higher sedimentation rates over the shorter, recent time scale is due to salt marsh accretion keeping up with sea level rise as it has rapidly increased on a short time scale.

Site Location	Accretion Rates Compared to Local Sea Level Rise	Consistent with the Sadler Effect
Gull Island	Keeping up	No
Shark Island	Keeping up	Yes
SE Corner of Gull Island	Keeping up	Yes
Near the Wetlands Institute	Keeping up	Yes

Table 10. Each site location accretion rates compared to Relative Sea Level Rise and Consistency with the Sadler Effect (Sadler 1981).

Boyd et al. (2017) found that salt marsh accretion rates were lower than RSLR in Barnegat Bay, NJ, which is a similar estuary to SMIL with back-barrier and mainland coastal marshes. Using two different models, Boyd et al. (2017) estimated that the accretion rate based on the ^{210}Pb chronology is 3.0 ± 0.8 mm/yr and 2.8 ± 0.6 mm/yr based on the ^{137}Cs chronology. The Barnegat accretion rates results are not consistent with the accretion rates from the SMIL site.

Conclusion

In this study, the accretion rates of salt marshes on Gull Island, Shark Island and near the Wetlands Institute were determined using radionuclide dating of ^{210}Pb . Radionuclide methods are used to gain insight on sediment accretion rates in order to compare accretion rates to local RSLR. Accretion dates were calculated at time intervals for the dating of the entire core, since the beginning of the local sea level record (1911) and since the year of the observed peak in ^{241}Am and ^{137}Cs based on ^{210}Pb chronology. The different time scales for accretion rate calculation allow for a greater understanding of the rate over time and demonstrate how accretion rates differ from year to year. The accretion rates for the study sites vary based on time scale. The accretion rates from the age since the year of observed peak in ^{241}Am and ^{137}Cs based on ^{210}Pb chronology are: (1) Gull Island: 4.3 ± 0.2 ; (2) Shark Island: 4.1 ± 0.1 ; (3) southeast corner of Gull Island: 5.2 ± 0.1 and; (4) near The Wetlands Institute: 6.0 ± 0.2 . The accretion indicates that the salt marsh is keeping up with the rate of local RSLR in the study site (4.21 ± 0.2 mm/year). Under current conditions, the salt marshes are not in immediate risk of flooding from sea level rise. The increase in accretion rates over time found in the Shark Island, southeast corner of Gull Island and near the Wetlands Institute samples also indicates that the marshes have kept up with sea level rise on a short time scale, demonstrating the resiliency of the salt marsh

ecosystem. However, salt marsh accretion must continue to grow at the same rate in order to match sea level rise. Without human intervention on salt marsh sediment, the future accretion rates of the salt marsh islands are based on sediment transport relative to local channels and water flows. The discrepancies in accretion rate of Gull Island, Shark Island and near the Wetland Institute demonstrates the dynamic sediment deposition within the system resulting in different accretion rates based on location.

The results of this study regarding the dynamics of the SMIL salt marsh islands provide data to inform the decision on where to place dredged material. USACE initiatives look to promote the beneficial use of dredged material, such as lateral deposition to build up salt marshes. Since the marsh system is keeping up with sea level rise naturally, lateral deposition of sediment on the system is likely not necessary. However, future work could aim to sample more cores within the salt marsh system to develop a more comprehensive view of accretion rates in the area. The measurement of accretion rates in other back barrier salt marsh systems will also provide a fuller understanding of salt marsh accretion rates compared to sea level rise.

Appendix

Appendix A

LOI Data for Gull Island, Shark Island, southeast corner of Gull Island and near the Wetland

Institute cores.

Gull Island

Depth (cm)	Volume (cm ³)	Crucible ID	Crucible Mass	Crucible + Wet Sediment	Wet Sediment Weight	Dry Sediment + Crucible Mass	Dry Sediment + Crucible Mass (2)
2	1.4	C1	23.611	26.271	2.66	24.712	24.692
4	1.6	C2	28.092	30.074	1.982	29.182	28.88
6	1.2	C3	24.899	26.341	1.442	25.533	25.518
8	1.8	C4	28.723	30.783	2.06	29.627	29.6
10	1.5	C5	27.843	29.96	2.117	28.753	28.744
12	2.3	C6	24.847	28.321	3.474	26.279	26.255
14	2	C7	25.546	27.816	2.27	26.332	26.162
16	2	C8	25.986	28.522	2.536	26.807	26.484
18	2	C9	28.228	30.678	2.45	29.063	28.973
20	2	C10	26.861	29.321	2.46	27.699	27.637
22	2	C11	26.692	29.254	2.562	27.657	27.616
24	2	C12	30.056	32.671	2.615	30.939	30.569
26	2	C13	24.518	27.296	2.778	25.522	25.489
28	1.4	C14	28.954	30.813	1.859	29.621	29.612
30	2	C15	24.767	27.035	2.268	25.484	25.474
32	1.4	C16	27.281	29.777	2.496	28.366	27.949
34	2	C17	25.238	27.674	2.436	26.135	26.126
36	2	C18	25.165	27.9	2.735	26.174	26.131
38	2	C19	23.91	26.542	2.632	24.837	24.825
40	2	C20	25.279	27.806	2.527	25.93	25.515
42	2	C21	28.116	30.621	2.505	29.152	29.092
44	2	C22	26.347	28.971	2.624	27.351	26.982
46	2	C23	28.911	31.542	2.631	30.036	29.818
48	2	C24	27.821	30.352	2.531	28.737	28.593
50	2	C25	9.678	12.54	2.862	N/A	10.96
52	2	C26	8.991	11.941	2.95	N/A	10.245
54	1.4	C27	8.776	11.086	2.31	N/A	9.797
56	2	C28	9.142	11.701	2.559	N/A	10.055

Depth (cm)	Volume (cm ³)	Crucible ID	Crucible Mass	Crucible + Wet Sediment	Wet Sediment Weight	Dry Sediment + Crucible Mass	Dry Sediment + Crucible Mass (2)
58	2	C29	9.143	12.19	3.047	N/A	10.279

Dry Sediment Mass (1) (oven)	Dry Sediment Mass (2) (g) (oven)	Mass of Crucible + Ash (after furnace)	Mass of Ash inorganic	Organic Content (g)	Water content	LOI (%)	Boyd method P _s (density of unconsolidated solids)	P _d (dry-bulk density) ((kg m ⁻³))	Dry-bulk Density (M/V; kg/m ³)
1.101	1.081	24.518	0.907	0.174	59.36%	16.10	2373.385754	539.554	772.142
1.09	0.788	28.547	0.455	0.333	60.24%	42.26	1988.794416	502.933	492.5
0.634	0.619	25.419	0.52	0.099	57.07%	15.99	2374.894992	579.856	515.833
0.904	0.877	29.45	0.727	0.15	57.43%	17.10	2358.574686	572.589	487.222
0.91	0.901	28.627	0.784	0.117	57.44%	12.99	2419.112098	575.863	600.667
1.432	1.408	26.011	1.164	0.244	59.47%	17.33	2355.255682	536.728	612.174
0.786	0.616	25.914	0.368	0.248	72.86%	40.26	2018.181818	319.702	308
0.821	0.498	26.287	0.301	0.197	80.36%	39.56	2028.493976	221.970	249
0.835	0.745	28.532	0.304	0.441	69.59%	59.19	1739.838926	354.801	372.5
0.838	0.776	27.494	0.633	0.143	68.46%	18.4	2339.110825	391.380	388
0.965	0.924	27.45	0.758	0.166	63.93%	17.97	2345.909091	462.056	462
0.883	0.513	30.229	0.173	0.34	80.38%	66.28	1635.730994	216.054	256.5
1.004	0.971	25.332	0.814	0.157	65.05%	16.17	2372.317199	445.235	485.5
0.667	0.658	29.489	0.535	0.123	64.60%	18.69	2335.212766	450.925	470
0.717	0.707	25.35	0.583	0.124	68.83%	17.54	2352.178218	386.135	353.5
1.085	0.668	27.809	0.528	0.14	73.24%	20.96	2301.916168	320.791	477.143
0.897	0.888	25.994	0.756	0.132	63.55%	14.86	2391.486486	470.099	444
1.009	0.966	25.926	0.761	0.205	64.68%	21.22	2298.043478	448.328	483
0.927	0.915	24.65	0.74	0.175	65.24%	19.13	2328.852459	440.702	457.5
0.651	0.236	25.333	0.054	0.182	90.66%	77.12	1476.355932	98.091	118
1.036	0.976	28.844	0.728	0.248	61.04%	25.41	2236.47541	504.283	488
1.004	0.635	26.797	0.45	0.185	75.80%	29.13	2181.732283	283.349	317.5
1.125	0.907	29.677	0.766	0.141	65.53%	15.55	2381.477398	437.942	453.5
0.916	0.772	27.987	0.166	0.606	69.50%	78.50	1456.088083	342.396	386
	1.282	10.817	1.139	0.143	55.21%	11.15	2446.029641	618.387	641
	1.254	10.084	1.093	0.161	57.49%	12.84	2421.267943	575.056	627
	1.021	9.669	0.893	0.128	55.80%	12.54	2425.710088	606.067	729.286
	0.913	9.887	0.745	0.168	64.32%	18.40	2339.507119	455.594	456.5
	1.136	10.122	0.979	0.157	62.72%	13.82	2406.839789	484.328	568

Shark Island

Depth (cm)	Volume (cm ³)	Crucible ID	Crucible Mass	Crucible + Wet Sediment	Wet Sediment Weight	Dry Sediment + Crucible Mass	Dry Sediment Weight
0-2	5	1	25.0165	30.9047	5.8882	26.6431	1.6266
2-4	5	2	25.8976	31.175	5.2774	27.4752	1.5776
4-6	5	3	21.6140	27.0566	5.4426	23.0596	1.4456
6-8	5	4	21.6848	26.5273	4.8425	22.8545	1.1697
8-10	5	5	24.9061	29.4446	4.5385	25.9893	1.0832
10-12	5	6	22.3458	27.8144	5.4686	23.6539	1.3081
12-14	5	7	22.5235	27.4911	4.9676	23.6149	1.0914
14-16	5	8	23.5377	28.8535	5.3158	24.6857	1.1480
16-18	5	9	23.5175	29.0724	5.5549	24.8112	1.2937
18-20	5	10	24.0302	28.9772	4.9470	25.1789	1.1487
20-22	5	11	24.4280	29.8244	5.3964	25.6132	1.1852
22-24	5	12	24.7354	29.5913	4.8559	25.8280	1.0926
24-26	5	13	23.8858	29.3203	5.4345	25.2638	1.3780
26-28	5	14	23.8008	29.6159	5.8151	25.4792	1.6784
28-30	5	15	23.1842	28.5062	5.3220	24.7723	1.5881
30-32	5	16	24.5938	29.9366	5.3428	26.1773	1.5835
32-34	5	17	23.3590	28.9986	5.6396	25.2692	1.9102
34-36	5	18	24.6816	29.7448	5.0632	25.8527	1.1711
36-38	5	19	23.5498	29.4610	5.9112	25.8012	2.2514
38-40	5	20	24.3261	30.3636	6.0375	26.6535	2.3274
40-42	5	21	23.2384	29.0438	5.8054	25.6483	2.4099
42-44	5	22	25.2550	30.9439	5.6889	27.8739	2.6189
44-46	5	23	25.6034	31.8951	6.2917	28.5383	2.9349
46-48	5	24	24.7962	30.7262	5.9300	26.9403	2.1441
48-50	5	25	25.2936	30.8848	5.5912	27.3279	2.0343
50-52	5	26	23.9639	29.5191	5.5552	25.9998	2.0359
52-54	5	27	24.3354	30.6903	6.3549	26.4816	2.1462
54-56	5	28	25.8423	31.5929	5.7506	27.8298	1.9875
56-58	5	29	24.4789	29.8768	5.3979	26.1858	1.7069
58-60	5	30	24.8685	29.9641	5.0956	26.3249	1.4564
60-62	5	31	26.1739	31.8460	5.6721	27.7672	1.5933
62-64	5	32	24.1462	28.7788	4.6326	25.4415	1.2953
64-66	5	33	24.9457	30.1201	5.1744	26.5620	1.6163
66-68	5	34	24.0676	29.2137	5.1461	25.5120	1.4444
68-70	5	35	9.0369	14.3944	5.3575	10.6386	1.6017

Depth (cm)	Volume (cm ³)	Crucible ID	Crucible Mass	Crucible + Wet Sediment	Wet Sediment Weight	Dry Sediment + Crucible Mass	Dry Sediment Weight
70-72	5	36	8.9987	14.5734	5.5747	10.9449	1.9462
72-74	5	37	26.5422	32.1112	5.5690	28.3756	1.8334
74-76	5	38	24.7002	29.7963	5.0961	26.0323	1.3321
76-78	5	39	28.6877	34.7052	6.0175	30.4741	1.7864
78-80	5	40	8.7780	13.8769	5.0989	10.4690	1.6910
80-82	5	41	9.8113	15.7254	5.9141	12.1197	2.3084

Mass of Crucible + Ash	Mass of Ash (inorganic)	Organic Content (g)	Water content (%)	LOI (% solid mass)	Boyd method p_s (density of unconsolidated solids)	P_d (dry-bulk density) ((kg m ⁻³))	Dry-Bulk density (M/V; Kg/m ³)
26.1265	1.1100	0.5166	72.38%	31.76%	2143.135374	329.4699596	325.32
26.9538	1.0562	0.5214	70.11%	33.05%	2124.162018	361.0111791	315.52
22.5455	0.9315	0.5141	73.44%	35.56%	2087.222607	313.4960429	289.12
22.4289	0.7441	0.4256	75.85%	36.39%	2075.13465	280.8768481	233.94
25.5831	0.6770	0.4062	76.13%	37.50%	2058.75	276.7717996	216.64
23.1976	0.8518	0.4563	76.08%	34.88%	2097.224983	278.1622803	261.62
23.1993	0.6758	0.4156	78.03%	38.08%	2050.230896	251.9084497	218.28
24.3180	0.7803	0.3677	78.40%	32.03%	2139.164634	248.3377531	229.6
24.4241	0.9066	0.3871	76.71%	29.92%	2170.147639	271.0010856	258.74
24.7900	0.7598	0.3889	76.78%	33.86%	2112.321755	269.1656179	229.74
25.2714	0.8434	0.3418	78.04%	28.84%	2186.066487	253.7473087	237.04
25.5316	0.7962	0.2964	77.50%	27.13%	2211.21911	261.1609887	218.52
24.9395	1.0537	0.3243	74.64%	23.53%	2264.048621	300.5056068	275.6
25.1045	1.3037	0.3747	71.14%	22.32%	2281.824952	350.3132985	335.68
24.5191	1.3349	0.2532	70.16%	15.94%	2375.629368	366.8359758	317.62
25.8691	1.2753	0.3082	70.36%	19.46%	2323.890748	362.6068547	316.7
24.9670	1.6080	0.3022	66.13%	15.82%	2377.441106	428.3206056	382.04
25.5401	0.8585	0.3126	76.87%	26.69%	2217.615063	269.5980492	234.22
25.5638	2.0140	0.2374	61.91%	10.54%	2454.995114	499.7438185	450.28
26.3814	2.0553	0.2721	61.45%	11.69%	2438.139985	506.8453657	465.48
25.3832	2.1448	0.2651	58.49%	11.00%	2448.29329	558.7215291	481.98
27.6098	2.3548	0.2641	53.96%	10.08%	2461.759517	642.8899568	523.78
28.2768	2.6734	0.2615	53.35%	8.91%	2479.022795	655.8619972	586.98
26.6672	1.8710	0.2731	63.84%	12.74%	2422.761998	466.4485588	428.82

Mass of Crucible + Ash	Mass of Ash (inorganic)	Organic Content (g)	Water content (%)	LOI (% solid mass)	Boyd method p_s (density of unconsolidated solids)	P_d (dry-bulk density) ((kg m ⁻³))	Dry-Bulk density (M/V; Kg/m ³)
27.0754	1.7818	0.2525	63.62%	12.41%	2427.541661	470.3404229	406.86
25.7786	1.8147	0.2212	63.35%	10.86%	2450.284886	475.5467842	407.18
26.2028	1.8674	0.2788	66.23%	12.99%	2419.041096	428.0937768	429.24
27.5970	1.7547	0.2328	65.44%	11.71%	2437.815849	441.2163615	397.5
25.9257	1.4468	0.2601	68.38%	15.24%	2385.99918	393.8385834	341.38
26.0605	1.1920	0.2644	71.42%	18.15%	2343.131008	347.6388961	291.28
27.5072	1.3333	0.2600	71.91%	16.32%	2370.120505	341.0997352	318.66
25.1326	0.9864	0.3089	72.04%	23.85%	2259.437968	336.8661931	259.06
26.2470	1.3013	0.3150	68.76%	19.49%	2323.512343	386.3085511	323.26
25.2024	1.1348	0.3096	71.93%	21.43%	2294.912767	339.1796851	288.88
10.3373	1.3004	0.3013	70.10%	18.81%	2333.474433	366.642705	320.34
10.6618	1.6631	0.2831	65.09%	14.55%	2396.169458	445.3989305	389.24
28.1084	1.5662	0.2672	67.08%	14.57%	2395.761972	414.0824203	366.68
25.7045	1.0043	0.3278	73.86%	24.61%	2248.265896	311.0423051	266.42
30.0862	1.3985	0.3879	70.31%	21.71%	2290.803292	362.503601	357.28
10.1745	1.3965	0.2945	66.84%	17.42%	2353.988764	416.5605761	338.2
11.8312	2.0199	0.2885	60.97%	12.50%	2426.28184	514.5311343	461.68

Southeast corner of Gull Island

Depth (cm)	Volume (cm ³)	Crucible ID	Crucible Mass	Crucible + Wet Sediment	Wet Sediment Weight	Dry Sediment + Crucible Mass	Dry Sediment Weight
0-2	5	1	24.9054	31.3333	6.4279	27.1318	2.2264
2-4	5	2	23.8855	29.6878	5.8023	26.2296	2.3441
4-6	5	3	21.6145	27.4071	5.7926	23.8956	2.2811
6-8	5	4	21.6850	28.5675	6.8825	24.2751	2.5901
8-10	5	5	26.1741	32.2923	6.1182	28.4521	2.2780
10-12	5	6	23.9637	28.7701	4.8064	25.1579	1.1942
12-14	5	7	24.5937	29.5893	4.9956	26.0339	1.4402
14-16	5	8	22.3456	27.8682	5.5226	23.8877	1.5421
16-18	5	9	23.5170	28.8560	5.3390	24.8621	1.3451
18-20	5	10	25.2544	29.8137	4.5593	26.3083	1.0539
20-22	5	11	24.4287	29.8587	5.4300	25.9265	1.4978

Depth (cm)	Volume (cm ³)	Crucible ID	Crucible Mass	Crucible + Wet Sediment	Wet Sediment Weight	Dry Sediment + Crucible Mass	Dry Sediment Weight
22-24	5	12	24.7350	31.1833	6.4483	27.1158	2.3808
24-26	5	13	25.0165	30.4894	5.4729	26.8158	1.7993
26-28	5	14	23.8006	28.9379	5.1373	25.2587	1.4581
28-30	5	15	23.1839	28.7562	5.5723	24.7415	1.5576
30-32	5	16	23.5372	28.9303	5.3931	25.3036	1.7664
32-34	5	17	23.3582	29.2566	5.8984	25.2563	1.8981
34-36	5	18	23.6806	30.2026	6.5220	25.9640	2.2834
36-38	5	19	23.5493	29.6208	6.0715	25.8707	2.3214
38-40	5	20	24.3259	30.5592	6.2333	27.0096	2.6837
40-42	5	21	25.2929	31.2433	5.9504	28.0852	2.7923
42-44	5	22	24.4787	30.8327	6.3540	27.4544	2.9757
44-46	5	23	25.6021	30.9735	5.3714	27.6334	2.0313
46-48	5	24	23.2377	29.5132	6.2755	25.4179	2.1802
48-50	5	25	22.5231	27.4088	4.8857	24.1137	1.5906
50-52	5	26	25.8976	32.1232	6.2256	27.7665	1.8689
52-54	5	27	24.3354	30.9494	6.6140	26.4063	2.0709
54-56	5	28	25.8413	31.8007	5.9594	27.8982	2.0569
56-58	5	29	24.7961	30.9008	6.1047	27.0672	2.2711
58-60	5	30	24.8679	30.8936	6.0257	26.9113	2.0434
60-62	5	31	24.1457	29.9007	5.7550	25.9871	1.8414
62-64	5	32	24.0294	29.5594	5.5300	25.8319	1.8025
64-66	5	33	24.9442	30.7135	5.7693	26.8987	1.9545
66-68	5	34	24.0668	29.7108	5.6440	26.0912	2.0244
68-70	5	35	9.4954	15.1571	5.6617	11.5066	2.0112
70-72	5	36	9.0358	14.6782	5.6424	10.9120	1.8762
72-74	5	37	26.5365	32.3807	5.8442	28.5405	2.0040
74-76	5	38	24.6988	30.4227	5.7239	26.3661	1.6673
76-78	5	39	28.6864	34.3860	5.6996	30.3783	1.6919
78-80	5	40	8.9991	14.9620	5.9629	10.8913	1.8922
82-84	5	41	9.8094	15.5948	5.7854	11.7940	1.9846
84-86	5	42	8.7775	14.3331	5.5556	10.3111	1.5336
86-88	5	43	8.7329	14.4397	5.7068	10.3593	1.6264
88-90	5	44	9.6796	15.7017	6.0221	11.3484	1.6688
90-92	5	45	9.1432	14.5366	5.3934	10.8245	1.6813
92-94	5	46	9.4713	15.0334	5.5621	10.5441	1.0728
94-96	5	47	9.4770	15.5015	6.0245	10.8231	1.3461

Mass of Crucible + Ash	Mass of Ash inorganic	organic content (g)	Water content (%)	LOI (% solid mass)	Boyd method p_s (density of unconsolidated solids)	P_d (dry-bulk density) ((kg m ⁻³))	Dry-Bulk density (M/V; Kg/m ³)
26.6387	1.7333	0.4931	65.36%	22.15%	2284.426428	437.0875138	445.28
25.7856	1.9001	0.444	59.60%	18.94%	2331.56478	533.262845	468.82
23.4054	1.7909	0.4902	60.62%	21.49%	2294.102407	514.1110298	456.22
23.7701	2.0851	0.5050	62.37%	19.50%	2323.389444	486.5838576	518.02
28.0159	1.8418	0.4362	62.77%	19.15%	2328.518876	480.2658541	455.6
24.6678	0.7041	0.4901	75.15%	41.04%	2006.711606	288.6998847	238.84
25.6495	1.0558	0.3844	71.17%	26.69%	2217.64616	348.2854745	288.04
23.4730	1.1274	0.4147	72.08%	26.89%	2214.68906	335.329786	308.42
24.4192	0.9022	0.4429	74.81%	32.93%	2125.974277	295.7377537	269.02
25.8728	0.6184	0.4355	76.88%	41.32%	2002.55622	265.9386539	210.78
25.5276	1.0989	0.3989	72.42%	26.63%	2218.503806	330.622825	299.56
26.7555	2.0205	0.3603	63.08%	15.13%	2387.536542	477.6001025	476.16
26.5068	1.4903	0.3090	67.12%	17.17%	2357.551826	412.2319595	359.86
24.9324	1.1318	0.3263	71.62%	22.38%	2281.036966	343.3824578	291.62
24.3977	1.2138	0.3438	72.05%	22.07%	2285.535439	337.3265821	311.52
25.0395	1.5023	0.2641	67.25%	14.95%	2390.215693	411.3071235	353.28
24.9473	1.5891	0.3090	67.82%	16.28%	2370.692271	401.9256729	379.62
25.5794	1.8988	0.3846	64.99%	16.84%	2362.403433	445.7982238	456.68
25.5424	1.9931	0.3283	61.77%	14.14%	2402.10778	499.9817042	464.28
26.5962	2.2703	0.4134	56.95%	15.40%	2383.559638	582.6630469	536.74
27.7048	2.4119	0.3804	53.07%	13.62%	2409.739283	656.2501236	558.46
27.0808	2.6021	0.3736	53.17%	12.56%	2425.441073	655.595264	595.14
27.3207	1.7186	0.3127	62.18%	15.39%	2383.706986	492.2253988	406.26
25.0838	1.8461	0.3341	65.26%	15.32%	2384.733052	442.3001117	436.04
23.7983	1.2752	0.3154	67.44%	19.83%	2318.513768	406.1244844	318.12
27.3944	1.4968	0.3721	69.98%	19.91%	2317.321419	368.0555584	373.78
26.0476	1.7122	0.3587	68.69%	17.32%	2355.381718	388.3005341	414.18
27.6125	1.7712	0.2857	65.48%	13.89%	2405.819437	439.4194462	411.38
26.7886	1.9925	0.2786	62.80%	12.27%	2429.672405	483.9163556	454.22
26.6231	1.7552	0.2882	66.09%	14.10%	2402.672017	429.7655448	408.68
25.6931	1.5474	0.2940	68.00%	15.97%	2375.298143	399.2548506	368.28
25.5178	1.4884	0.3141	67.41%	17.43%	2353.840777	407.7886858	360.5
26.5999	1.6557	0.2988	66.12%	15.29%	2385.269378	428.6744208	390.9
25.7844	1.7176	0.3068	64.13%	15.16%	2387.219917	460.4421884	404.88

Mass of Crucible + Ash	Mass of Ash inorganic	organic content (g)	Water content (%)	LOI (% solid mass)	Boyd method p_s (density of unconsolidated solids)	P_d (dry-bulk density) ((kg m ⁻³))	Dry-Bulk density (M/V; Kg/m ³)
11.1413	1.6459	0.3653	64.48%	18.16%	2342.999702	453.247743	402.24
10.5378	1.5020	0.3742	66.75%	19.94%	2316.814839	416.732223	375.24
28.2598	1.7233	0.2807	65.71%	14.01%	2404.097305	435.7962833	400.8
26.0413	1.3425	0.3248	70.87%	19.48%	2323.635219	355.1528572	333.46
30.0613	1.3749	0.317	70.32%	18.74%	2334.575921	363.5498887	338.38
10.5380	1.5389	0.3533	68.27%	18.67%	2335.530599	394.1211114	378.44
11.3888	1.5794	0.4052	65.70%	20.42%	2309.866976	432.8029871	396.92
10.0252	1.2477	0.2859	72.40%	18.64%	2335.956573	333.4162157	306.72
10.0624	1.3295	0.2969	71.50%	18.26%	2341.650885	346.4151425	325.28
11.0414	1.3618	0.307	72.29%	18.40%	2339.572148	335.0173879	333.76
10.5609	1.4177	0.2636	68.83%	15.68%	2379.528341	386.8719573	336.26
11.1893	1.7180	0.6548	75.32%	47.70%	1908.81	284.4213874	214.56
10.4199	0.9429	0.4032	77.66%	29.95%	2169.687988	258.5134855	269.22

Near the Wetlands Institute

Depth (cm)	Volume (cm ³)	Crucible ID	Crucible Mass	Crucible + Wet Sediment	Wet Sediment Weight	Dry Sediment + Crucible Mass	Dry Sediment Weight
0-2	5	1	24.1473	28.3826	4.2353	25.2617	1.1144
2-4	5	2	26.5367	32.2931	5.7564	28.0102	1.4735
4-6	5	3	23.5575	29.4314	5.8739	25.1717	1.6142
6-8	5	4	24.947	28.9259	3.9789	25.9039	0.9569
8-10	5	5	24.4296	28.3272	3.8976	25.3357	0.9061
10-12	5	6	21.6157	25.8862	4.2705	22.5105	0.8948
12-14	5	7	23.1848	28.9249	5.7401	24.3532	1.1684
14-16	5	8	24.3266	28.7462	4.4196	25.2612	0.9346
16-18	5	9	24.4783	29.4482	4.9699	25.5302	1.0519
18-20	5	10	24.4464	29.659	5.2126	25.9386	1.4922
20-22	5	11	23.9647	29.2199	5.2552	25.1274	1.1627
22-24	5	12	28.6861	33.3981	4.712	30.4811	1.795
24-26	5	13	22.5238	28.2197	5.6959	25.8324	3.3086
26-28	5	14	25.0174	30.5298	5.5124	27.2457	2.2283
28-30	5	15	25.8981	30.9985	5.1004	27.2876	1.3895
30-32	5	16	23.5378	28.0226	4.4848	24.7562	1.2184
32-34	5	17	24.8684	30.6584	5.79	26.4752	1.6068

Depth (cm)	Volume (cm ³)	Crucible ID	Crucible Mass	Crucible + Wet Sediment	Wet Sediment Weight	Dry Sediment + Crucible Mass	Dry Sediment Weight
34-36	5	18	24.0299	29.6168	5.5869	25.5909	1.561
36-38	5	19	26.174	31.6672	5.4932	27.7972	1.6232
38-40	5	20	24.0679	29.1345	5.0666	25.5456	1.4777
40-42	5	21	25.8419	31.681	5.8391	27.8086	1.9667
42-44	5	22	25.255	30.3212	5.0662	27.2071	1.9521
44-46	5	23	23.6813	29.6107	5.9294	25.7655	2.0842
46-48	5	24	23.8012	29.9085	6.1073	25.9635	2.1623
48-50	5	25	24.3359	30.5238	6.1879	26.3677	2.0318
50-52	5	26	23.239	28.8986	5.6596	25.5578	2.3188
52-54	5	27	23.359	30.3028	6.9438	26.0256	2.6666
54-56	5	28	23.8862	30.5523	6.6661	26.1989	2.3127
56-58	5	29	21.6854	28.6069	6.9215	24.7941	3.1087
58-60	5	30	25.6031	31.4913	5.8882	27.8669	2.2638
60-62	5	31	24.5937	30.263	5.6693	26.542	1.9483
62-64	5	32	22.3459	28.4778	6.1319	25.0269	2.681
64-66	5	33	23.5183	30.0479	6.5296	26.0291	2.5108
66-68	5	34	24.6985	32.481	7.7825	27.9553	3.2568
68-70	5	35	25.2937	31.7895	6.4958	27.5694	2.2757
70-72	5	36	25.7876	32.0799	6.2923	28.5023	2.7147
72-74	5	37	24.7356	32.4994	7.7638	28.3612	3.6256
74-76	5	38	25.8422	32.5567	6.7145	29.0653	3.2231
76-78	5	39	23.8875	31.2865	7.399	27.6283	3.7408
78-80	5	40	16.4139	23.3204	6.9065	19.7022	3.2883
80-82	5	41	24.0324	31.7435	7.7111	28.0879	4.0555
82-84	5	42	25.0171	32.0743	7.0572	28.6827	3.6656
84-86	5	43	26.1755	33.6367	7.4612	30.1437	3.9682
86-88	5	44	25.8983	34.4174	8.5191	30.115	4.2167
88-90	5	45	23.5386	32.7512	9.2126	29.0315	5.4929
90-92	5	46	24.8696	33.8409	8.9713	30.7532	5.8836
92-94	5	47	23.1846	30.8856	7.701	26.6464	3.4618
94-96	5	48	24.3275	33.2458	8.9183	30.2922	5.9647
96-98	5	49	24.1465	33.8648	9.7183	30.8479	6.7014
98-100	5	50	23.5499	31.3722	7.8223	29.3825	5.8326
100-102	5	51	24.4798	34.135	9.6552	31.6976	7.2178
102-104	5	52	23.9854	33.9246	9.9392	30.7568	6.7714
104-106	5	53	23.2402	32.3118	9.0716	29.0789	5.8387
106-108	5	54	24.0731	33.4443	9.3712	30.6142	6.5411

Depth (cm)	Volume (cm ³)	Crucible ID	Crucible Mass	Crucible + Wet Sediment	Wet Sediment Weight	Dry Sediment + Crucible Mass	Dry Sediment Weight
108-110	5	55	24.9469	34.123	9.1761	31.5588	6.6119
110-112	5	56	24.4308	32.6031	8.1723	29.9221	5.4913
112-114	5	57	21.6169	31.0493	9.4324	28.4282	6.8113
114-116	5	58	25.9078	33.8308	7.923	31.327	5.4192
116-118	5	59	25.2554	36.2672	11.0118	33.4375	8.1821

Mass of Crucible + Ash	Mass of Ash inorganic	Organic Content (g)	Water Content (%)	LOI (% solid mass)	Boyd method p_s (density of unconsolidated solids)	P_d (dry-bulk density) ((kg m ⁻³))	Dry-Bulk density (M/V; Kg/m ³)
24.9573	0.8100	0.3044	73.69%	27.32%	2208.467337	312.6552523	222.88
27.5683	1.0316	0.4419	74.40%	29.99%	2169.149644	302.0568964	294.7
24.4479	0.8904	0.7238	72.52%	44.84%	1950.85863	322.6072707	322.84
25.2916	0.3446	0.6123	75.95%	63.99%	1669.3782	270.6201484	191.38
25.0761	0.6465	0.2596	76.75%	28.65%	2188.841188	270.735702	181.22
22.1543	0.5386	0.3562	79.05%	39.81%	2024.825659	238.5227333	178.96
23.8976	0.7128	0.4556	79.64%	38.99%	2036.795618	231.1052568	233.68
24.9153	0.5887	0.3459	78.85%	37.01%	2065.945859	241.5579893	186.92
25.1481	0.6698	0.3821	78.83%	36.32%	2076.026238	241.9347993	210.38
25.9064	1.46	0.0322	71.37%	2.16%	2578.279051	353.0823856	298.44
25.6665	1.7018	0.4609	58.85%	21.31%	2296.743	544.2203548	232.54
30.1624	1.4763	0.3187	61.91%	17.75%	2349.003343	495.3148194	359
25.5941	3.0703	0.2383	41.91%	7.20%	2504.124101	903.5568964	661.72
26.9285	1.9111	0.3172	59.58%	14.24%	2400.744514	537.2146726	445.66
26.959	1.0609	0.3286	72.76%	23.65%	2262.36272	326.7629432	277.9
24.379	0.8412	0.3772	72.83%	30.96%	2154.908076	323.3751714	243.68
26.1067	1.2383	0.3685	72.25%	22.93%	2272.873413	334.1844615	321.36
25.2644	1.2345	0.3265	72.06%	20.92%	2302.533632	337.520109	312.2
27.4994	1.3254	0.2978	70.45%	18.35%	2340.306801	361.6996021	324.64
25.2597	1.1918	0.2859	70.83%	19.35%	2325.589768	355.7347163	295.54
27.4571	1.6152	0.3515	66.32%	17.87%	2347.273097	424.3757484	393.34
26.9011	1.6461	0.306	61.47%	15.68%	2379.571231	503.9762136	390.42
25.371	1.6897	0.3945	64.85%	18.93%	2331.756549	446.9044691	416.84
25.6595	1.8583	0.3040	64.59%	14.06%	2403.331175	453.5637208	432.46
26.0312	1.6953	0.3365	67.16%	16.56%	2366.543459	411.8658573	406.36
25.2632	2.0242	0.2946	59.03%	12.70%	2423.238744	547.8953215	463.76
25.6287	2.2697	0.3969	61.60%	14.88%	2391.203405	502.3260749	533.32

Mass of Crucible + Ash	Mass of Ash inorganic	Organic Content (g)	Water Content (%)	LOI (% solid mass)	Boyd method p_s (density of unconsolidated solids)	P_d (dry-bulk density) ((kg m ⁻³))	Dry-Bulk density (M/V; Kg/m ³)
25.8513	1.9651	0.3476	65.31%	15.03%	2389.058244	441.6855883	462.54
24.4914	2.806	0.3027	55.09%	9.74%	2466.863319	621.9611031	621.74
27.5882	1.9851	0.2787	61.55%	12.31%	2429.025974	504.7140713	452.76
26.2471	1.6534	0.2949	65.63%	15.14%	2387.496792	436.4390963	389.66
24.8146	2.4687	0.2123	56.28%	7.92%	2493.5953	601.3381902	536.2
25.7644	2.2461	0.2647	61.55%	10.54%	2455.025888	505.9324	502.16
27.7155	3.017	0.2398	58.15%	7.36%	2501.76308	567.5090893	651.36
27.3271	2.0334	0.2423	64.97%	10.65%	2453.485082	449.3088093	455.14
28.3218	2.5342	0.1805	56.86%	6.65%	2512.259918	591.6916208	542.94
28.1014	3.3658	0.2598	53.30%	7.17%	2504.664056	658.6493378	725.12
28.8638	3.0216	0.2015	52.00%	6.25%	2518.099345	685.3409724	644.62
27.4058	3.5183	0.2225	49.44%	5.95%	2522.565494	737.916927	748.16
19.4941	3.0802	0.2081	52.39%	6.33%	2516.971079	677.4822992	657.66
27.8879	3.8555	0.2	47.41%	4.93%	2537.505856	782.5910711	811.1
28.5059	3.4888	0.1768	48.06%	4.82%	2539.098647	768.6694318	733.12
29.97	3.7945	0.1737	46.82%	4.38%	2545.653697	796.2958761	793.64
29.8791	3.9808	0.2359	50.50%	5.59%	2527.761994	716.3711403	843.34
28.8422	5.3036	0.1893	40.38%	3.45%	2559.339875	948.1990131	1098.58
30.5782	5.7086	0.175	34.42%	2.97%	2566.276769	1105.97793	1176.72
26.3903	3.2057	0.2561	55.05%	7.40%	2501.251083	624.8617109	692.36
30.1141	5.7866	0.1781	33.12%	2.99%	2566.107264	1142.640515	1192.94
30.6916	6.5451	0.1563	31.04%	2.33%	2575.714478	1205.394297	1340.28
29.2933	5.7434	0.0892	25.44%	1.53%	2587.518774	1387.124098	1166.52
31.5773	7.0975	0.1203	25.24%	1.67%	2585.499321	1393.060366	1443.56
30.5708	6.5854	0.186	31.87%	2.75%	2569.621349	1179.509583	1354.28
28.899	5.6588	0.1799	35.64%	3.08%	2564.70687	1072.094924	1167.74
30.452	6.3789	0.1622	30.20%	2.48%	2573.548333	1230.391875	1308.22
31.4247	6.4778	0.1341	27.94%	2.03%	2580.186028	1302.455367	1322.38
29.7675	5.3367	0.1546	32.81%	2.82%	2568.614172	1152.115217	1098.26
28.2804	6.6635	0.1478	27.79%	2.17%	2578.102124	1306.927785	1362.26
31.1993	5.2915	0.1277	31.60%	2.36%	2575.360385	1188.693443	1083.84
33.2818	8.0264	0.1557	25.70%	1.90%	2582.026864	1376.743398	1636.42

Appendix B

Subsampling Data sent to Fallout RadioNuclide Analytics Lab at Dartmouth College.

Gull Island

Length	ID Code	Pan	Weight of Pan	Weight Wet (sample + pan)	Sample Wet Weight	Sample + Pan Dry Weight	Sample Dry Weight	Container Mass	Mass of sample + plastic	Dry Mass
0-3	SMIL-GC 1-01	A	16.163	166.125	149.962	75.873	59.71	22.553	81.715	59.162
3-6	SMIL-GC 1-02	B	16.124	179.84	163.716	83.544	67.42	20.876	80.375	59.499
6-9	SMIL-GC 1-03	C	16.163	172.82	156.657	76.077	59.914	21.264	72.987	51.723
9-12	SMIL-GC 1-04	D	16.311	162.77	146.459	73.266	56.955	21.245	70.78	49.535
12-15	SMIL-GC 1-05	E	16.211	170.785	154.574	73.266	57.055	22.569	70.629	48.06
15-18	SMIL-GC 1-06	F	16.176	149.794	133.618	63.04	46.864	21.951	68.386	46.435
18-21	SMIL-GC 1-07	G	16.326	141.615	125.289	54.47	38.144	21.149	58.71	37.561
21-24	SMIL-GC 1-08	H	16.416	150.17	133.754	60.752	44.336	21.254	65.425	44.171
24-27	SMIL-GC 1-09	I	16.397	156.89	140.493	60.892	44.495	22.588	66.909	44.321
27-30	SMIL-GC 1-10	J	16.186	157.312	141.126	61.851	45.665	21.958	67.595	45.637
30-33	SMIL-GC 1-11	K	16.314	160.355	144.041	63.049	46.735	21.931	68.516	46.585
33-36	SMIL-GC 1-12	L	16.105	157.751	141.646	61.322	45.217	21.216	66.109	44.893
36-39	SMIL-GC 1-13	A	16.704	177.841	161.137	76.495	59.791	22.27	82.528	60.258
39-42	SMIL-GC 1-14	I	17.021	176.024	159.003	75.81	58.789	21.97	81.485	59.515
42-45	SMIL-GC 1-15	D	17.272	159.094	141.822	73.083	55.811	22.117	78.921	56.804
45-48	SMIL-GC K	K	17.112	170.574	153.462	76.77	59.658	22.694	83.365	60.671

Length	ID Code	Pan	Weight of Pan	Weight Wet (sample + pan)	Sample Wet Weight	Sample + Pan Dry Weight	Sample Dry Weight	Container Mass	Mass of sample + plastic	Dry Mass
	1-16									
48-51	SMIL-GC 1-17	J	16.821	159.72	142.899	70.802	53.981	19.765	74.235	54.47
51-54	SMIL-GC 1-18	L	16.85	164.027	147.177	74.908	58.058	21.725	80.255	58.53
54-57	SMIL-GC 1-19	H	16.965	160.885	143.92	74.527	57.562	21.87	80.203	58.333
57-61*	SMIL-GC 1-20	G	16.815	198.963	182.148	85.304	68.489	21.867	91	69.133
61-64	SMIL-GC 1-21	B	16.805	155.962	139.157	66.556	49.751	22.549	72.797	50.248
64-67	SMIL-GC 1-22	F	16.895	171.892	154.997	72.921	56.026	21.232	77.498	56.266
67-70	SMIL-GC 1-23	E	16.801	161.416	144.615	68.42	51.619	20.208	72.065	51.857
70-73	SMIL-GC 1-24	C	16.987	169.723	152.736	68.984	51.997	21.632	74.211	52.579

Shark Island

Length	ID Code	Pan	Pan Mass	Wet Sample + Pan Mass	Sample Wet Weight	Dry Sample + Pan Mass	Sample Dry Weight	Container Mass	Sample + Container Mass	Dry Mass
0-3	SMIIL-GC 2-01	A	16.065	95.210	79.145	38.118	22.053	21.999	43.994	21.995
3-6	SMIIL-GC 2-02	B	16.033	128.488	112.455	45.847	29.814	22.018	51.559	29.541
6-9	SMIIL-GC 2-03	C	16.018	173.717	157.699	56.685	40.667	21.781	55.184	33.403
9-12	SMIIL-GC 2-04	D	16.447	149.669	133.222	45.838	29.391	21.923	51.698	29.775
12-15	SMIIL-GC 2-05	E	16.176	153.408	137.232	43.649	27.473	20.807	48.214	27.407
15-18	SMIIL-GC 2-06	F	16.001	139.214	123.213	42.998	26.997	20.986	48.327	27.341
18-21	SMIIL-GC 2-06	G	15.956	141.961	126.005	41.213	25.257	20.970	46.555	25.585

Length	ID Code	Pan	Pan Mass	Wet Sample + Pan Mass	Sample Wet Weight	Dry Sample + Pan Mass	Sample Dry Weight	Container Mass	Sample + Container Mass	Dry Mass
	2-07									
21-24	SMIIL-GC 2-08	H	16.125	143.955	127.830	44.531	28.406	21.336	50.000	28.664
24-27	SMIIL-GC 2-09	I	16.234	153.029	136.795	52.232	35.998	21.636	57.959	36.323
27-30	SMIIL-GC 2-10	J	15.938	147.224	131.286	54.602	38.664	21.497	60.489	38.992
30-33	SMIIL-GC 2-11	K	16.126	169.495	153.369	66.333	50.207	21.807	72.480	50.673
33-36	SMIIL-GC 2-12	L	16.058	162.195	146.137	66.420	50.362	21.0519	72.1245	51.0726
36-39	SMIIL-GC 2-13	M	13.617	160.875	147.258	75.883	62.266	21.3675	82.637	61.2695
39-42	SMIIL-GC 2-14	N	13.683	179.908	166.225	87.299	73.616	21.0035	94.233	73.2295
42-45	SMIIL-GC 2-15	O	13.647	146.341	132.694	66.595	52.948	20.7823	73.2982	52.5159
45-48	SMIIL-GC 2-16	P	13.652	204.611	190.959	93.795	80.143	21.1586	99.144	77.9854
48-51	SMIIL-GC 2-17	Q	13.643	159.016	145.373	68.296	54.653	20.8471	74.4815	53.6344
51-54	SMIIL-GC 2-18	R	13.585	159.108	145.523	67.184	53.599	21.0823	73.0318	51.9495
54-57	SMIIL-GC 2-19	S	13.603	123.954	110.351	50.036	36.433	19.8886	55.885	35.9964
57-60	SMIIL-GC 2-20	T	13.602	150.409	136.807	57.807	44.205	21.7045	64.8986	43.1941
60-63	SMIIL-GC 2-21	U	13.618	132.494	118.876	47.105	33.487	21.8948	55.4992	33.6044
63-66	SMIIL-GC 2-22	V	13.571	162.587	149.016	57.306	43.735	21.1445	64.2422	43.0977
66-69	SMIIL-GC 2-23	A	16.002	157.285	141.283	58.008	42.006	21.5638	62.8733	41.3095
69-72	SMIIL-GC 2-24	C	16.063	156.787	140.724	63.858	47.795	21.2608	66.749	45.4882
72-75	SMIIL-GC 2-25	I	16.141	128.137	111.996	51.555	35.414	21.7422	55.7763	34.0341

Length	ID Code	Pan	Pan Mass	Wet Sample + Pan Mass	Sample Wet Weight	Dry Sample + Pan Mass	Sample Dry Weight	Container Mass	Sample + Container Mass	Dry Mass
75-78	SMIIL-GC 2-26	L	15.993	151.925	135.932	63.607	47.614	22.0893	69.2361	47.1468
78-81	SMIIL-GC 2-27	B	16.032	162.128	146.096	67.105	51.073	20.5332	70.8507	50.3175
81-84	SMIIL-GC 2-28	D	16.128	166.499	150.371	67.869	51.741	20.8476	70.869	50.0214
84-87	SMIIL-GC 2-29	E	16.025	145.086	129.061	62.618	46.593	20.0402	65.7145	45.6743

Southeast corner of Gull Island

Length	ID Code	Pan	Pan Mass	Wet Sample + Pan Mass	Sample Wet Weight	Dry Sample + Pan Mass	Sample Dry Weight	Container Mass	Sample + Container Mass	Dry Mass
0-4	Gull-2021 -01	1	9.017	158.912	149.895	68.663	59.646	20.4518	41.7506	21.2988
4-8	Gull-2021 -02	2	9.003	196.577	187.574	83.458	74.455	21.0436	34.605	13.5614
8-12	Gull-2021 -03	3	8.984	164.541	155.557	60.728	51.744	21.2498	60.8426	39.5928
12-16	Gull-2021 -04	4	8.947	154.433	145.486	47.967	39.020	21.1787	53.8061	32.6274
16-20	Gull-2021 -05	5	9.055	175.057	166.002	49.895	40.840	20.4052	46.8955	26.4903
20-24	Gull-2021 -06	6	9.221	178.644	169.423	60.972	51.751	22.0601	47.0079	24.9478
24-28	Gull-2021 -07	7	9.223	179.625	170.402	59.579	50.356	20.720	67.3541	46.634
28-32	Gull-2021 -08	8	9.138	170.184	161.046	57.869	48.731	21.4158	69.482	48.066
32-36	Gull-2021 -09	9	9.224	195.644	186.420	85.829	76.605	21.4046	72.7227	51.3181
36-40	Gull-2021 -10	10	9.216	192.693	183.477	91.764	82.548	14.3612	62.8757	48.5145
40-44	Gull-2021 -11	A	15.98 2	221.871	205.889	102.331	86.349	21.22	74.852	53.632
44-48	Gull-2021	B	16.00	193.136	177.133	80.452	64.449	21.7297	81.048	59.3183

Length	ID Code	Pan	Pan Mass	Wet Sample + Pan Mass	Sample Wet Weight	Dry Sample + Pan Mass	Sample Dry Weight	Container Mass	Sample + Container Mass	Dry Mass
	-12		3							
48-52	Gull-2021-13	C	15.998	214.868	198.870	81.905	65.907	21.2384	87.072	65.8336
52-56	Gull-2021-14	D	16.084	192.866	176.782	73.775	57.691	21.0825	78.6039	57.5214
56-60	Gull-2021-15	E	16.042	190.691	174.649	78.125	62.083	20.0126	80.6405	60.6279
60-64	Gull-2021-16	F	15.975	231.545	215.570	86.257	70.282	21.6459	80.3469	58.701
64-68	Gull-2021-17	G	16.034	178.331	162.297	75.462	59.428	21.3419	80.7989	59.457
68-72	Gull-2021-18	H	16.055	203.413	187.358	80.401	64.346	20.9153	85.142	64.2267
72-76	Gull-2021-19	I	16.103	187.573	171.470	62.372	46.269	22.0147	76.8504	54.8357
76-80	Gull-2021-20	J	15.923	169.176	153.253	71.449	55.526	21.3006	67.6404	46.3398
80-84	Gull-2021-21	K	16.994	208.865	191.871	71.679	54.685	20.6698	75.8874	55.2176
84-88	Gull-2021-22	L	15.997	201.205	185.208	70.884	54.887	20.9854	75.3353	54.3499
88-92	Gull-2021-23	M	13.585	207.351	193.766	75.04	61.455	21.227	82.306	61.079
92-96	Gull-2021-24	N	13.656	159.795	146.139	55.813	42.157	20.6921	62.6217	41.9296

Near the Wetlands Institute

Length	ID Code	Pan	Pan Mass	Wet Sample + Pan Mass	Sample Wet Weight	Dry Sample + Pan Mass	Sample Dry Weight	Container Mass	Sample + Container Mass	Dry Mass
0-4	TWI-2021-01	1	9.006	96.123	87.117	33.339	24.333	20.8599	45.4908	24.6309
4-8	TWI-2021-02	2	8.999	164.042	155.043	50.523	41.524	22.2874	41.3859	19.0985
8-12	TWI-2021-03	3	9.186	158.385	149.199	43.785	34.599	21.446	48.7815	27.3355

Length	ID Code	Pan	Pan Mass	Wet Sample + Pan Mass	Sample Wet Weight	Dry Sample + Pan Mass	Sample Dry Weight	Container Mass	Sample + Container Mass	Dry Mass
	21-03									
12-16	TWI-20 21-04	4	9.166	164.433	155.267	43.648	34.482	20.9208	44.829	23.9082
16-20	TWI-20 21-05	5	8.919	162.658	153.739	42.211	33.292	23.2919	44.5058	21.2139
20-24	TWI-20 21-06	6	9.098	154.589	145.491	44.079	34.981	20.9256	40.2653	19.3397
24-28	TWI-20 21-07	7	9.203	218.808	209.605	127.884	118.681	20.877	94.247	73.370
28-32	TWI-20 21-08	8	9.205	204.904	195.699	92.905	83.7	20.6854	82.462	61.777
32-36	TWI-20 21-09	9	8.998	170.125	161.127	57.005	48.007	21.6844	48.6563	26.9719
36-40	TWI-20 21-10	10	8.951	184.733	175.782	65.268	56.317	21.5318	60.739	39.2072
40-44	TWI-20 21-11	11	16.02 9	181.582	165.553	71.459	55.43	20.4926	59.564	39.071
44-48	TWI-20 21-12	12	15.93 8	205.875	189.937	84.390	68.452	21.3035	69.3771	48.0736
48-52	TWI-20 21-13	13	13.61 6	197.299	183.683	83.063	69.447	21.6885	80.713	59.0245
52-56	TWI-20 21-14	14	15.99 1	243.775	227.784	108.815	92.824	21.6634	79.7028	58.0394
56-60	TWI-20 21-15	15	16.02 1	200.210	184.189	93.345	77.324	21.6556	78.0753	56.4197
60-64	TWI-20 21-16	16	15.99 6	205.436	189.440	93.637	77.641	21.2507	86.791	65.5403
64-68	TWI-20 21-17	17	13.54 5	198.123	184.578	88.951	75.406	22.0448	87.4	65.3552
68-72	TWI-20 21-18	18	13.60 1	193.114	179.513	91.614	78.013	21.0014	93.732	72.7306
72-76	TWI-20 21-19	19	13.62 2	206.627	193.005	100.622	87	20.3067	100.441	80.1343
76-80	TWI-20 21-20	20	13.67 7	205.985	192.308	102.292	88.615	21.2479	103.539	82.2911
80-84	TWI-20 21-21	21	16.13 4	203.707	187.573	107.358	91.224	21.4469	111.525	90.0781

Length	ID Code	Pan	Pan Mass	Wet Sample + Pan Mass	Sample Wet Weight	Dry Sample + Pan Mass	Sample Dry Weight	Container Mass	Sample + Container Mass	Dry Mass
84-88	TWI-20 21-22	22	13.65	200.522	186.872	117.556	103.906	22.5767	105.93	83.3533
88-92	TWI-20 21-23	23	16.04 2	226.800	210.758	143.788	127.746	21.3304	123.504	102.1736
92-96	TWI-20 21-24	24	13.73 7	240.565	226.828	157.347	143.61	21.8494	115.321	93.4716
96-100	TWI-20 21-25	25	16.10 7	240.15	224.043	169.869	153.762	21.9357	129.857	107.9213
100-104	TWI-20 21-26	26	16.02 5	256.805	240.78	186.019	169.994	22.9884	131.411	108.4226
104-108	TWI-20 21-27	27	15.93 4	276.706	260.772	197.787	181.853	20.6538	143.023	122.3692
108-112	TWI-20 21-28	28	16.06 2	250.759	234.697	181.811	165.749	22.5902	134.843	112.2528
112-116	TWI-20 21-29	29	13.68 1	263.606	249.925	191.832	178.151	21.1318	140.461	119.3292
116-118	TWI-20 21-30	30	16.11 9	288.575	272.456	216.548	200.429	21.1664	137.178	116.0116

References

- Blankespoor, B., Dasgupta, S., & Laplante, B. (2014). Sea-level rise and coastal wetlands. *Ambio*, 43(8), 996–1005. <https://doi.org/10.1007/s13280-014-0500-4>
- Boyd, B. M., Sommerfield, C. K., & Elsey-Quirk, T. (2017). Hydrogeomorphic influences on salt marsh sediment accumulation and accretion in two estuaries of the U.S. Mid-Atlantic coast. *Marine Geology*, 383, 132–145. <https://doi.org/10.1016/j.margeo.2016.11.008>
- Charlebois-Berg, J., Corrado, K., & Harby, O. (2023). *Estimates of Accretion Rates and Organic Content of Salt Marsh Islands in Southern New Jersey* [Paper]. Boston College.
- Costanza, R. (2008). Ecosystem services: Multiple classification systems are needed. *Biological Conservation*, 141(2), 350–352. <https://doi.org/10.1016/j.biocon.2007.12.020>
- de Groot, A. V., Veeneklaas, R. M., & Bakker, J. P. (2011). Sand in the salt marsh: Contribution of high-energy conditions to salt-marsh accretion. *Marine Geology*, 282(3), 240–254. <https://doi.org/10.1016/j.margeo.2011.03.002>
- From NYC to Miami, Major Cities Along the East Coast are Sinking—The New York Times*. (n.d.). Retrieved February 22, 2024, from <https://www.nytimes.com/interactive/2024/02/13/climate/flooding-sea-levels-groundwater.html>
- Hurricane Gloria—September 26-28, 1985*. (n.d.). Retrieved February 22, 2024, from <https://www.wpc.ncep.noaa.gov/tropical/rain/gloria1985.html>

Is the rate of sea-level rise increasing? (n.d.). NASA Sea Level Change Portal. Retrieved February 11, 2024, from

<https://sealevel.nasa.gov/faq/8/is-the-rate-of-sea-level-rise-increasing>

Landis, J. D. (2023). Age-Dating of Foliage and Soil Organic Matter: Aligning ^{228}Th : ^{228}Ra and ^7Be : ^{210}Pb Radionuclide Chronometers over Annual to Decadal Time Scales. *Environmental Science & Technology*, 57(40), 15047–15054.

<https://doi.org/10.1021/acs.est.3c06012>

Landis, J. D., Renshaw, C. E., & Kaste, J. M. (2016). Beryllium-7 and lead-210 chronometry of modern soil processes: The Linked Radionuclide Accumulation model, LRC. *Geochimica et Cosmochimica Acta*, 180, 109–125.

<https://doi.org/10.1016/j.gca.2016.02.013>

Ohenhen, L. O., Shirzaei, M., & Barnard, P. L. (2024). Slowly but surely: Exposure of communities and infrastructure to subsidence on the US east coast. *PNAS Nexus*, 3(1), pgad426. <https://doi.org/10.1093/pnasnexus/pgad426>

Sadler, P. M. (1981). Sediment Accumulation Rates and the Completeness of Stratigraphic Sections. *The Journal of Geology*, 89(5), 569–584.

Sea Level Trends—NOAA Tides & Currents. (n.d.-a). Retrieved February 11, 2024, from

<https://tidesandcurrents.noaa.gov/sltrends/>

Sea Level Trends—NOAA Tides & Currents. (n.d.-b). Retrieved February 22, 2024, from

https://tidesandcurrents.noaa.gov/sltrends/sltrends_station.shtml?id=8534720

Seven Mile Island Innovation Lab—The Wetlands Institute. (n.d.). Retrieved February 11, 2024, from <https://wetlandsinstitute.org/smiil-2-2/>

US EPA, O. (2017, November 2). *Wetlands* [Reports and Assessments].

<https://www.epa.gov/report-environment/wetlands>

Valiela, I., Lloret, J., Chenoweth, K., & Wang, Y. (2024). An example of accelerated changes in current and future ecosystem trajectories: Unexpected rapid transitions in salt marsh vegetation forced by sea level rise. *Environmental Challenges*, *14*, 100842.

<https://doi.org/10.1016/j.envc.2024.100842>

Wetlands' ability to overcome sea level rise threatened. (n.d.). Retrieved February 23, 2024,

from https://www.nsf.gov/news/news_summ.jsp?cntn_id=129792

Zeff, M. L. (1988a). Sedimentation in a salt marsh-tidal channel system, southern New

Jersey. *Marine Geology*, *82*(1), 33–48. [https://doi.org/10.1016/0025-3227\(88\)90005-9](https://doi.org/10.1016/0025-3227(88)90005-9)